Seventh International Conference on

Geochronology, Cosmochronology and Isotope Geology

ICOG 7

CANBERRA
1990

Excursion Guide A-1

Lady Elliot Island, Great Barrier Reef

20-22 September, 1990

by

A.R. Chivas, P.G. Flood, J.O.H. Stone & L.K. Ayliffe

Bureau of Mineral Resources, Geology and Geophysics
Record 1990/47

Seventh International Conference on

Geochronology, Cosmochronology and Isotope Geology

CANBERRA
1990

Excursion Guide A-1

Lady Elliot Island, Great Barrier Reef

20-22 September, 1990

by

A.R. Chivas[1], P.G. Flood[2], J.O.H. Stone[1] & L.K. Ayliffe[1]

[1] **Research School of Earth Sciences, The Australian National University, Canberra**

[2] **Department of Geology, The University of New England, Armidale, NSW**

Bureau of Mineral Resources, Geology and Geophysics
Record 1990/47

CONTENTS

Chapter 1: BACKGROUND TO THE GREAT BARRIER REEF

INTRODUCTION

The Great Barrier Reef is the largest carbonate province in the world, extending for 2300km along the continental shelf of northeastern Queensland. Its geological development is related to the northward drift of the Australian plate since its separation from Antarctica about 53 million years ago and to gradual subsidence of the eastern margin of Australia associated with sea floor spreading in the Tasman Sea. Reefs commenced growing in the Gulf of Papua more than 5 million years ago and progressively extended southwards along the shelf edge until the reefs east of Gladstone commenced their growth about 2 million years ago.

Both subsidence and glacial sea-level fluctuations have moulded the shape of the reefs which can be observed at various stages of development. Drilling has indicated that the reefs are composite structures up to 150 metres thick, of which only one fifth protrudes above the sea floor whilst the remaining four fifths is buried in sand and mud. Projections of the interplay of reef growth and sediment discharge from the coastal rivers indicate that the reefs could become buried in sand and mud within the next two million years.

The reefs of the Great Barrier Reef are a relatively recent phenomenon when compared to other areas of reef development such as the central Pacific and West Atlantic Oceans where reefs have been growing for the past 25 million years. During the past decade a considerable amount of new geological research concerning the development of the eastern margin of the Australian continent has revealed the reasons for this late development.

PHYSIOGRAPHY OF THE GREAT BARRIER REEF

The Great Barrier Reef province extends along the coast of Queensland from Torres Strait in the north to Lady Elliot Island, its southernmost coral cay, off Bundaberg, in the south. In places it extends up to 250km offshore, fronting onto the deep water of the Coral Sea and South Pacific Ocean. Behind the shelf-edge reefs is a protected area of shallow water referred to as the lagoon, which varies from 20 to 200km in width with water depths of 10 to 40m.

The bulk of the modern reef is submerged with cays and islands rising above sea level on only a small fraction of its area. Several types of islands are found on the reef. Near the coast, islands consist of rocky highpoints on the continental land surface stranded by Holocene sea level rise. Around these islands, coral growth is typically restricted to development of fringing reefs, due to inundation by sediment from coastal rivers. Islands

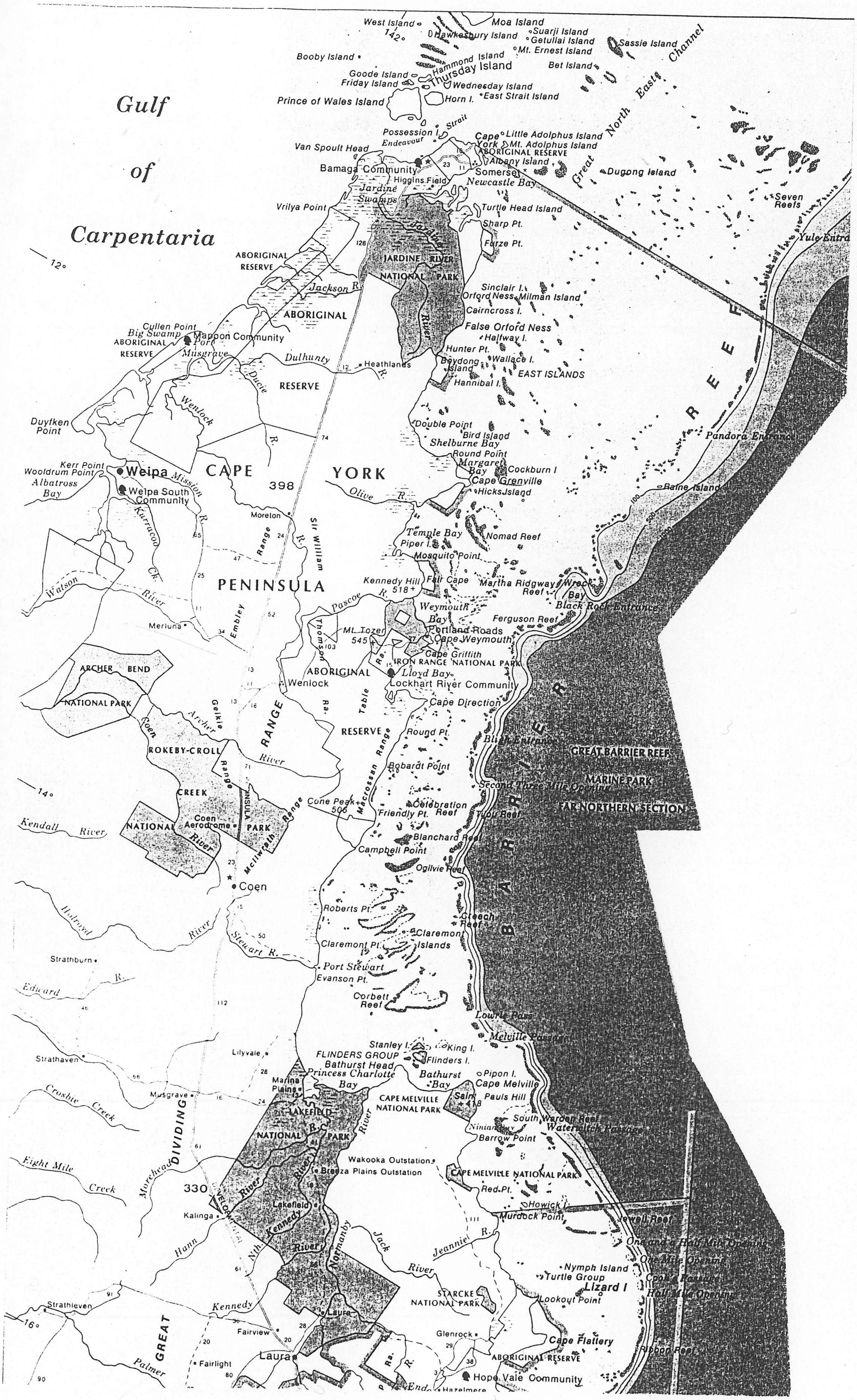

Figure 1(a): The Northern Great Barrier Reef

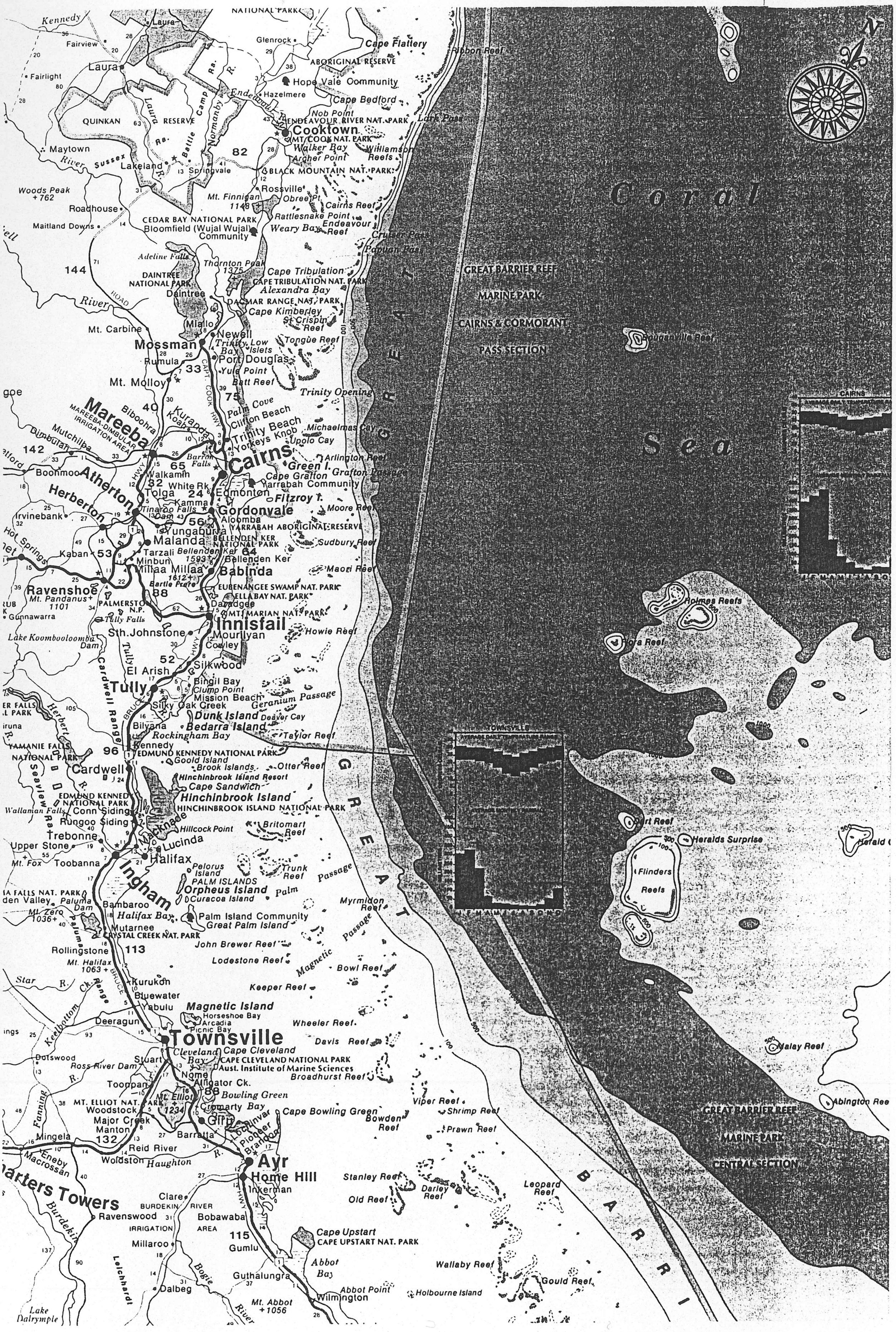

Figure 1(b): The Central Great Barrier Reef

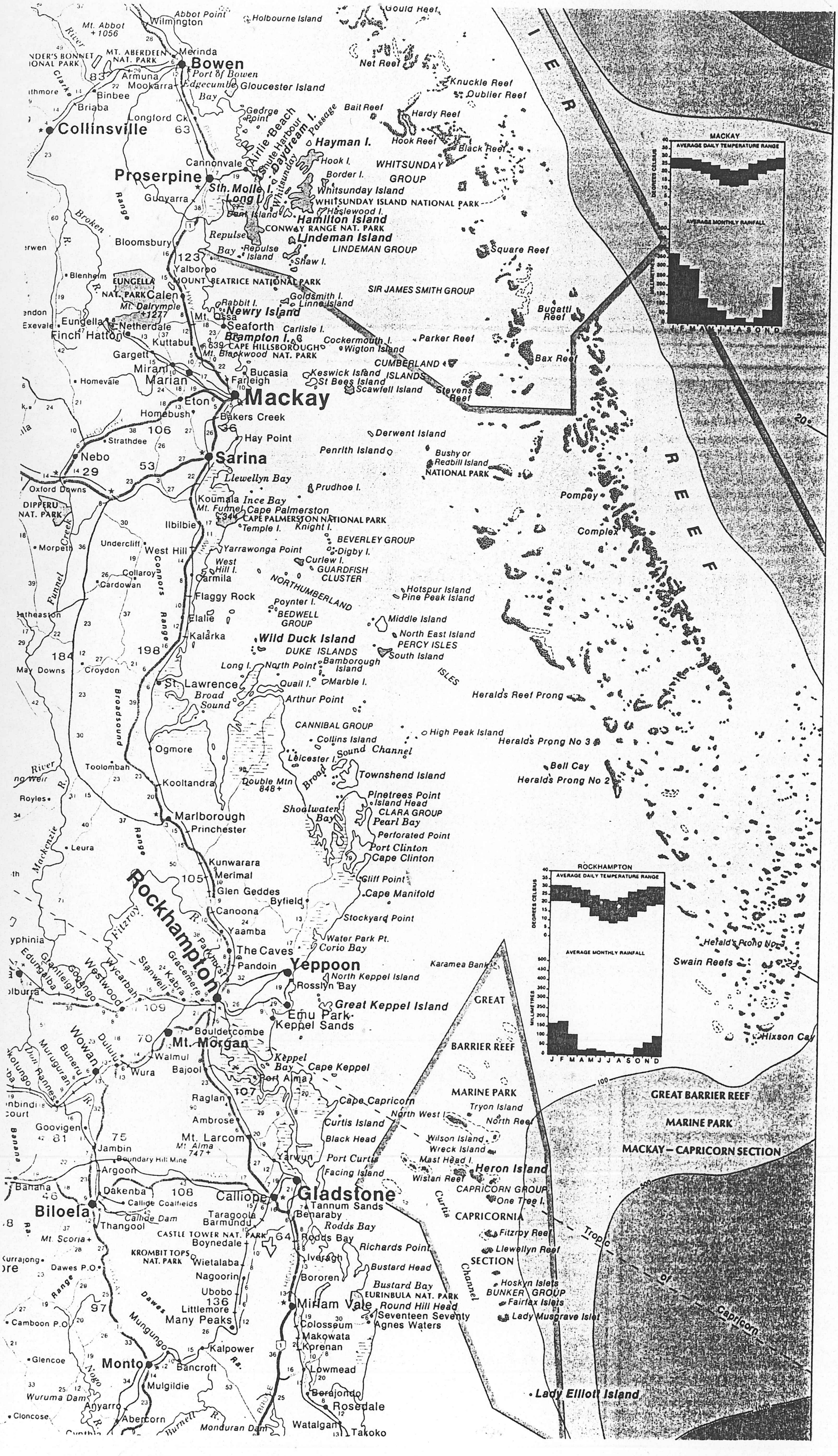

Figure 1(c): The Southern Great Barrier Reef further from the shore are typically low platforms no more than a few metres above sea level, constructed entirely from coralline sand and debris.

REGIONAL DIVISIONS OF THE REEF

Regional divisions of the Great Barrier Reefs have been recognised on the basis of water depth and type of reef development. The northermost 800km of the shelf edge is marked by a near continuous line of narrow reefs (ribbon reefs), separated by many small deep passages. Reef-fronts account for 71% of the distance. By contrast the central area has no true shelf-edge reef system, most of the reefs are situated several kilometres landward of the shelf-edge and they are separated from each other by wide expanses of deep water. Only 45% of the 640km of the central section is fronted by reefs. In the south, a strong shelf-edge reef system exists in the northeastern sector (Pompey Complex) but farther south the reefs are widely dispersed. Over a total of 800km of shelf edge in the southern section, reefs account for 36%.

THE LIVING REEF

The architects of the reef are tiny animals called coral polyps which by building a calcareous skeleton and dividing to form new polyps create a living structure or coral colony. Once the small larvae or planulae of the coral settle in an area where water depth, temperature and clarity, and wave and tidal action are conducive to continuing growth they begin the slow process of upward growth and deposit a hard calcareous structure. The coral colonies provide the framework around and within which live a myriad of reef-dwelling animals. An astonishing diversity and abundance of life forms has been identified from the Great Barrier Reef. There are around 400 different types of corals, about 4000 molluscs (clams, snails and their kin), countless thousands of sponges, worms, crustaceans (crabs, shrimp, etc), echinoderms (starfish, sea urchins, sea cucumbers) and other, less familiar, creatures. This immense variety of invertebrate life forms provides a backdrop to some 1500 species of fish.

After death corals may be bound together by the calcareous skeleton of marine plants known as coralline algae. The corals provide the framework and the coralline algae the mortar or cement of the solid structure. Should environmental conditions permit the corals to reach the water surface further upward growth is impossible as exposure to sun and drying will kill the coral polyp. Then expansion of the reef occurs by lateral growth. The direction of outward growth and the shape of the resultant reef are dependent on the physical conditions (winds, waves, currents) which mould the reef. However, some features of the reef's morphology may be inherited from the shape of the underlying platform on which the coral growth was initially established.

Over thousands of years coral growth, death, and cementation build a solid geological structure many metres thick with a veneer of living corals and associated plants and animals.

PRESENT REEF MORPHOLOGY

When observing the present-day morphological variations evident within the diversity of reef types it is important to realise that the reefs are at different stages of development. It has been demonstrated by shallow coring of modern reefs that the stage of development is closely correlated with the height of the limestone platform relative to the rising sea level. In general the rate of sea level rise (7 to 10m per 1 000 years) may outstrip the rate of coral reef growth (7-8m per 1 000 years). The oldest dated coral reef cores show that growth associated with the recent sea level rise commenced about 8 500 years before present in water depths ranging from 8 to 20m below the modern sea level. This means that a water depth in excess of 10m may have existed during the initial phase of recent reef growth on the pre-existing platforms. Once sea level stabilized about 6 500 years before present, reefs quickly caught up with sea level and began to grow laterally. Clearly reefs which commenced growth on the highest platforms would have reached modern sea level before those growing from lower platforms. Thus one tends to observe an across-the-shelf transition of more developed reef near to the shore to less developed reefs near the shelf edge. This is a direct response to the gradually increasing rate of subsidence of the shelf as one passes from the land to the edge of the continental shelf. Once reef growth reaches the level of mean low water, vertical growth ceases and the prevailing hydraulic regime (currents, waves, tides) modifies the growth. Subsequent evolution involves growth primarily to leeward (away from the wind direction), sediment infilling of back-reef lagoons replacement of the framebuilding organisms which dominated the initial phase of vertical growth by substrate-controlled organisms. Reefs may be observed at various stages of development, referred to as juvenile, adolescent, mature and senile.

When examining the concept of coral growth and reef development it is important to note that growth is the sum of both constructive and destructive processes operating over a time span of several thousand years. Rates of vertical growth of corals of up to 14m per thousand years have been recorded but such a linear measure of coral growth may be several times greater than the three-dimensional growth of the reef framework. Also it has been shown that different rates of growth will characterise different environments in the same reef. Finally, it should be noted that the reef framework constitutes only a few percent of the volume of a mature reef. The vast majority of the reef (as much as 90%) consists of debris infilling the fore-reef or back-reef (including the lagoon environments on some large platform reefs).

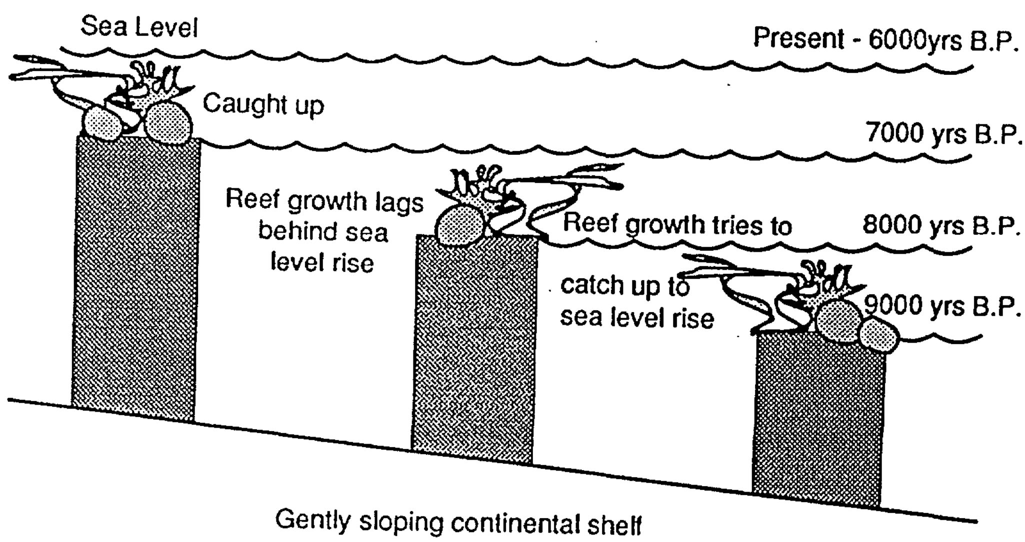

Figure 2

SEA LEVEL for past 10 000 years showing how the stages of morphological development of reefs is related to the height of the sub-reef platform. Senile reefs have been above or at the present level for several thousand years whereas young reefs have reached the present level only in the past 2 000 years. Young reefs have been shown to have developed on the deeper substrates.

GEOLOGIC HISTORY OF THE REEF

Drifting plates and glaciations

Prior to 53 million years ago Australia and Antarctica were joined as part of the Gondwana supercontinent. At this time the Australian landmass was situated south of latitude 40°S. Sea-floor spreading commenced between Australia and Antarctica, opening what is now the Southern Ocean along an E-W zone of weakness, and Australia commenced northward migration at a rate of a few centimetres per year. About 10 million years after the initial breakup the eastern portion of the Australian Plate (now represented by New Zealand and the large continental landmass underlying the tiny Lord Howe Island) was also removed by fracturing and sea-floor spreading along a N-S axis. Deep seismic studies have shown that sedimentation at the continental margin was dominated initially by non-marine alluvial and fluvial sediments which eventually gave way to an alternation of prograding deltaic sedimentation similar to that now occurring at the mouth of the Mississippi River, interspersed with onlapping marine sediments. This style of sedimentation continued for some 20 million years until about 30 million years ago when the earth began to experience the effects of world wide temperature fluctuations and sea-level oscillations associated with the great ice ages of the late Tertiary period.

Rises and falls in sea level associated with these glacial-interglacial cycles amounted to more than 100 metres. During glacial periods the continental landmass of northeastern Australia was exposed as the sea regressed, and rivers deposited their sediment load along the edge of the present continental margin. These periods of glaciation and lower sea level extended for some hundreds of thousands of years. With the rise in sea level following each interglacial warming, the shoreline migrated many kilometres westward across the continental shelf. Depending upon the gradient of the shelf, this landward transgression of the sea ranged from 20km to in excess of 250km at the southern end of the area now occupied by the Reef. Whilst the level of the sea fluctuated with each glacial event, the Australian continental mass continued its northward drift. Also the continental margin was gradually subsiding thus allowing a substantial thickness, in excess of 3km, of sediment to accumulate near the margin.

Initiation of the Reef

About 12 million years ago the northern tip of Australia passed beyond the Tropic of Capricorn where water temperatures would have been sufficient to allow coral larvae, originating from the already-flourishing Pacific coral reefs, to settle on rocky or sandy substrates, and the potential for coral reef growth existed for the first time. The sites first colonised were the levees or banks or bars and deltas of old rivers which had earlier flowed across the continental shelf during low sea level stands. Many of the present-day

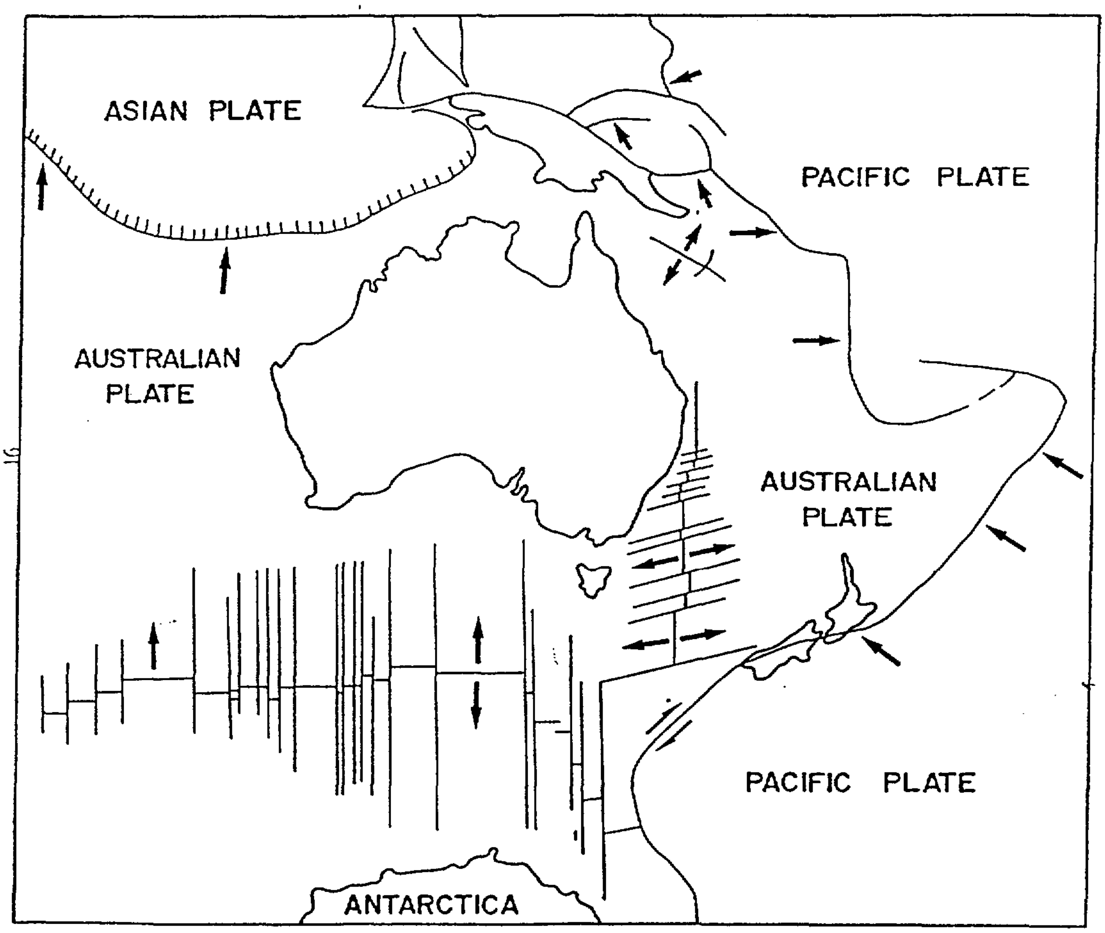

Figure 3

TECTONIC PLATES in the SW Pacific. Directions of sea floor spreading are indicated by the arrows. Australia's contact with Antarctica was severed about 50 million years ago.

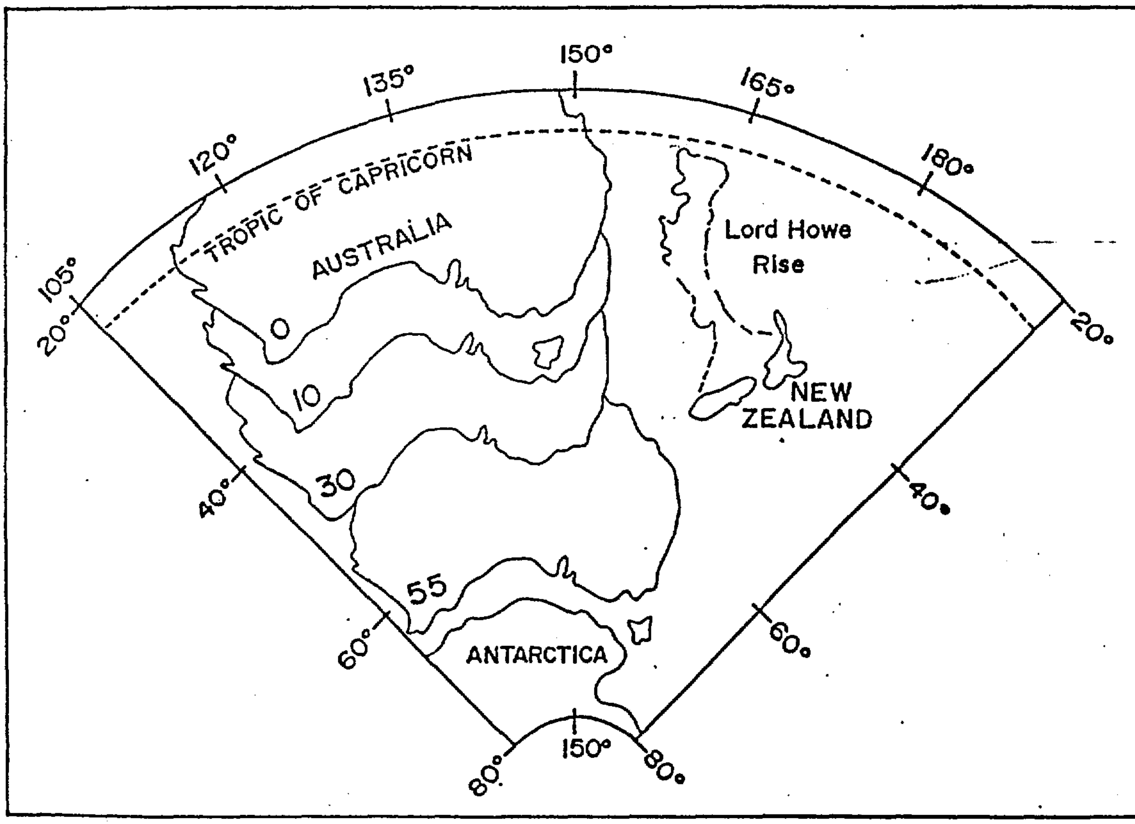

Figure 4

NORTHWARD DRIFT of the INDIAN-AUSTRALIAN PLATE at about 7cm per year for the past 50 million years has taken it through 27° of latitude. Sea water temperatures adequate to support coral reef development occur only north of the Tropic of Capricorn. The northern tip of the continent reached this latitude about 10 million years ago.

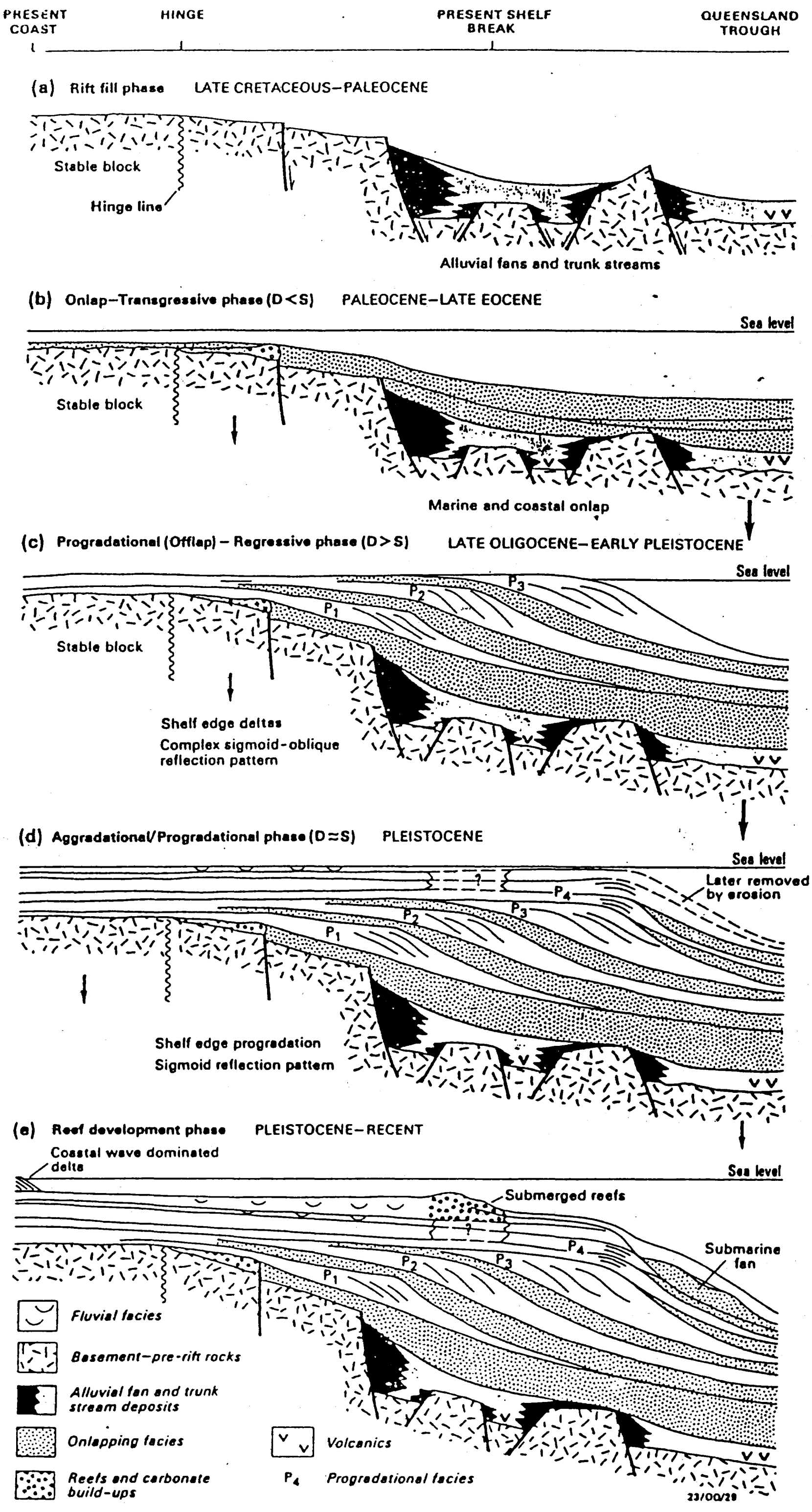

Figure 5

Development of passive margin, Queensland, (after Symonds *et al* (1983) Aust BMR Journal 8, p. 288).

reefs display morphological features which mimic the shape of substrates on which they developed. Once established the coral reefs flourished and in many instances were able to keep pace with rises of sea level during interglacial.periods. The corals, however, would have been killed during sea level falls and the hard calcareous skeletons which had been cemented into a resistant limestone mass of significant topographic relief, would have been left standing as pinnacles on the broad, flat continental shelf.

Dissolution by meteoric water will differentially lower the central area of a limestone platform or reef and subsequent coral growth associated with a later sea level rise will preferentially colonise the topographic elevations on the platform. Central lagoons, if present, would act as a trap for rain water and hence they would be leached preferentially with respect to outer margins of the reef. When sea level rose again the coral reef organisms would re-establish themselves on the limestone substrate of the earlier reef. In this instance the subsequent morphology would be strongly influenced by the shape of the pre-existing reef mass. Therefore the vertical record is one of superposition of reefs, separated by significant erosion surfaces and in some instances soil development at the contact.

Great Barrier Reef bores

Subsurface data within the Great Barrier Reef relies almost entirely on the results of two deep bores, drilled on Michaelmas Cay and Heron Island, on behalf of the Great Barrier Reef Committee in 1926 and 1937 respectively.

In each of these bores, drilled about 1100km apart, similar vertical sequences consisting of coralline material from the surface to depths of 124 and 155m in the northern and southern bores respectively, were encountered. The coralline material rested upon loosely coherent terrigenous sands. The results of these two bores have been largely overlooked because at the time they did not achieve the intended objective of proving Darwin's 1842 theory of coral reef development applicable to the Great Barrier Reef. As all the fossils in the bores appeared similar to present day forms it was suggested that there was no firm evidence of any sediment older than Recent (deposited within the past 20 000 years). As all the fossils appeared to be shallow-water forms it was concluded that subsidence of perhaps 200m had occurred. Although the Darwinian hypothesis of reef growth on a subsiding basement received support, the sub-reef material was unconsolidated sand and not volcanics, as required by Darwin's theory. These two findings confused reef researchers for almost 40 years. Earlier postulations concerning the expected age of the reef, made prior to drilling the bores, ranged from Pleistocene (2 million years) to Tertiary (5-6 million years), or even pre-Tertiary. Researchers were confused by the apparent young age of the Great Barrier Reef, which

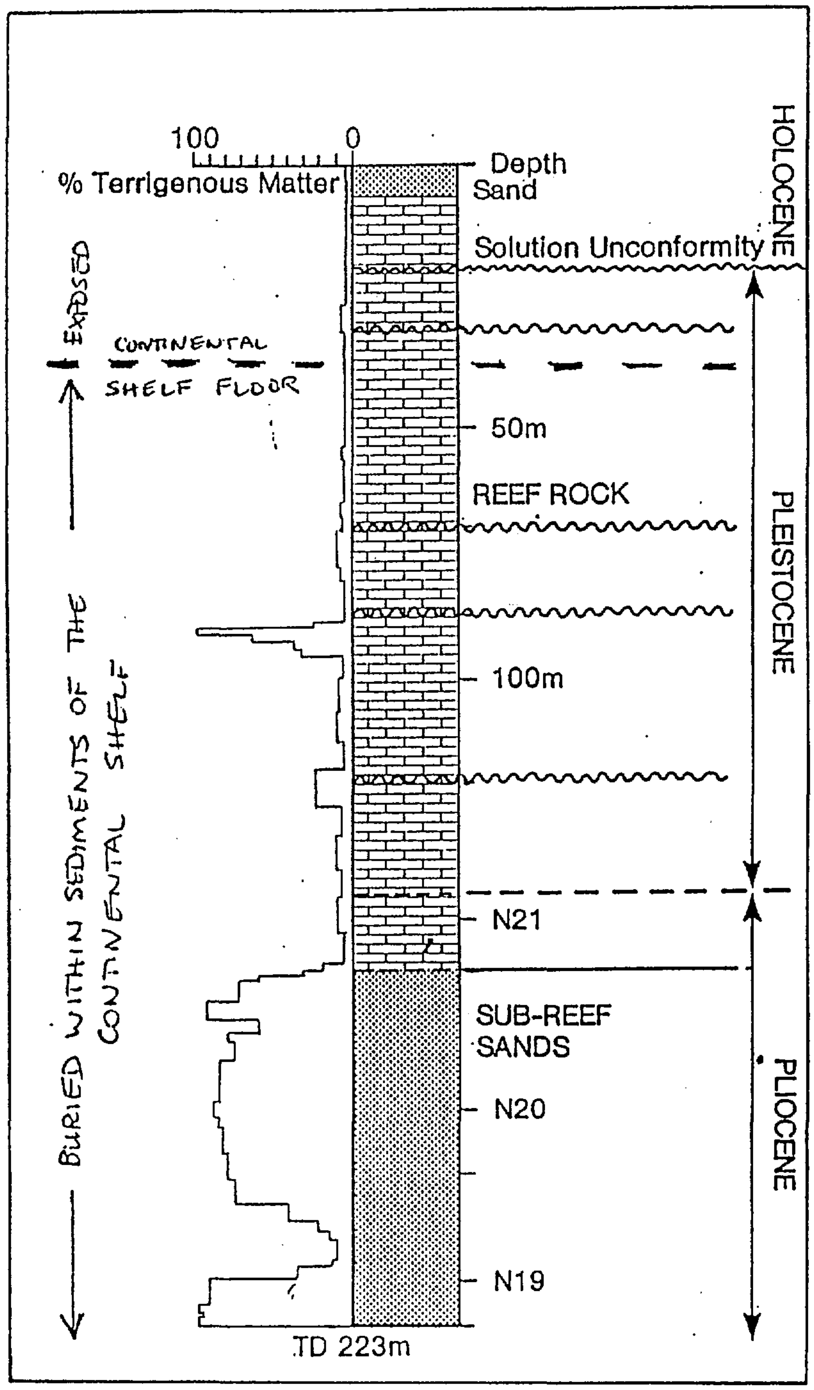

Figure 6

HERON ISLAND BORE (1937) encountered almost 150m of shallow water limestone resting on unconsolidated marine sands which contain fossils older than 2 million years. The limestone sequence contains at least 6 discrete phases of coral reef development separated by solution unconformities.

was at variance with ages obtained for reefs elsewhere. It was not until the early 1970s that a major breakthrough in the interpretation of the drilling results occurred, when researchers demonstrated that several major solution unconformities or erosion surfaces could be recognized in the drillcores. These features were identified as zones of calcite, formed by recrystallization of the pre-existing aragonitic skeletal material due to exposure to freshwater during subaerial exposure of the limestone. Subsequent studies of the microfossil content of the bores supported the suggestion of a much older age for the Reef. The time of commencement of reef growth has been established at the Heron Island drill site as being late Pliocene (prior to about 2 million years before present).

SEA LEVEL FLUCTUATIONS

The history of sea level fluctuations during the past 2 million years has been one of relatively brief periods (10 000 - 20 000 years) of high sea level alternating with longer (approximately 100 000 year) glacial periods of low sea level. Coral growth as we see it today has been possible for only ~5 percent of the time during the past 2 million years. The last period of extensive reef growth occurred between ~120 000 and ~140 000 years ago, coinciding with the last interglacial climax. In the intervening period until approximately 10 000 years before present, the continental shelf and reefs were exposed subaerially. In many instances it is possible to observe pre-Holocene or recent coral growth on top of more extensive older reefal masses. One excellent example can be seen underlying the modern reef growth of Heron Reef. Here the platform or reefal shoal extends to the east at a depth of approximately 15m. Subsurface scuba inspection by the writer (PGF) has shown the platform to be a pre-existing reef which developed during the 120 000 - 140 000 year sea level highstand, which was subject to subaerial solution during the intervening glacial period. Researchers have shown that one Pleistocene sea level was close to or slightly above (5m higher) the present level and that coral reef growth reached that level. Therefore the level at which this surface is now found is a function of gradual solution and erosion (2 to 4mm/year) during its 100 000 years of exposure combined with gradual subsidence (0.1mm/year) of the outer continental shelf on which the coral reefs are established.

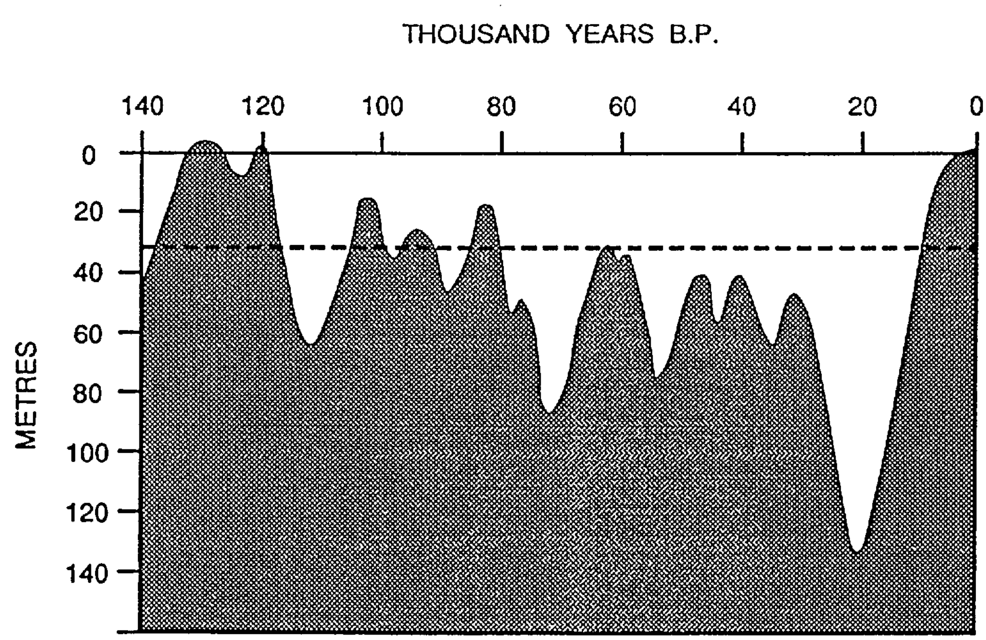

Figure 7

SEA LEVEL relative to present sea level for the past 140 000 years. Dashed line represents the general level below which the shelf is exposed, reefs are killed, and non-marine sedimentation prevails on the shelf. Coral reef development is generally restricted to the periods 83 000, 105 000 and 120 000 to 140 000 years before present.

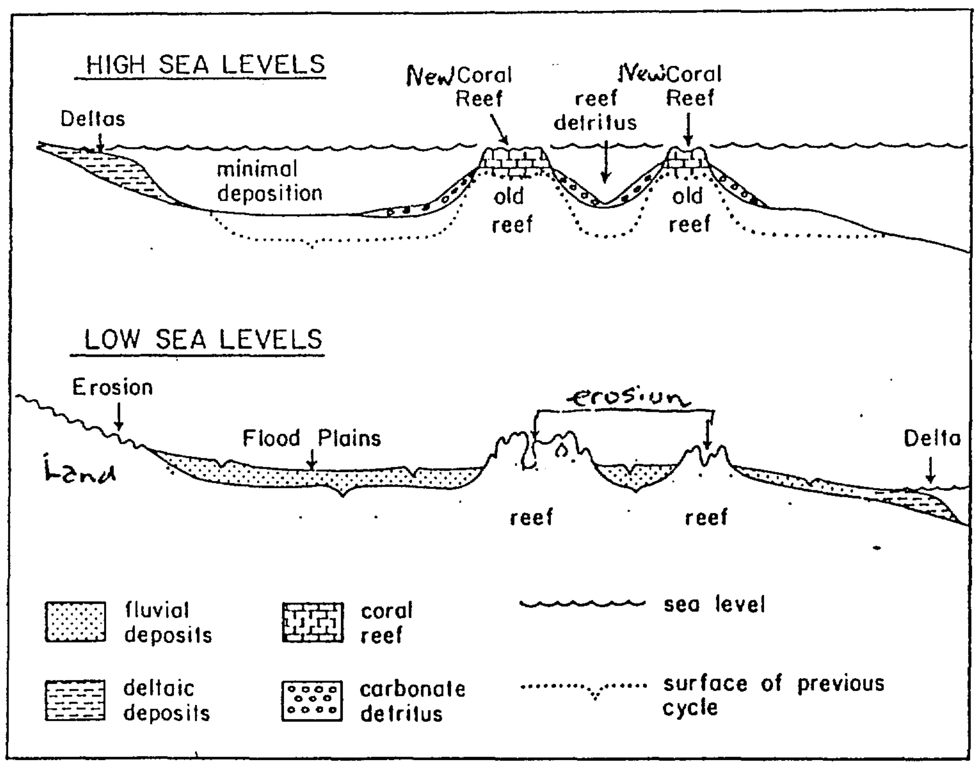

Figure 8

IDEALISED REPRESENTATION OF SHELF CONDITIONS at times of high and low sea levels during the last 2 million years when the sea level fluctuated some 150m in response to the glacial events.

Chapter 2:
RADIOCARBON EVIDENCE FOR THE TIMING AND RATE OF ISLAND DEVELOPMENT, BEACH-ROCK FORMATION AND PHOSPHATIZATION AT LADY ELLIOT ISLAND, QUEENSLAND

ALLAN CHIVAS[1], JOHN CHAPPELL[2], HENRY POLACH[2], BRAD PILLANS[3] and PETER FLOOD[4]

[1]Research School of Earth Sciences, The Australian National University, GPO Box 4, Canberra ACT 2601 (Australia)
[2]Research School of Pacific Studies, The Australian National University, GPO Box 4, Canberra ACT 2601 (Australia)
[3]Research School of Earth Sciences, Victoria University of Wellington, Private Bag, Wellington, (New Zealand)
[4]Department of Geology, The University of New England, Armidale NSW 2351 (Australia)

ABSTRACT

Chivas, A., Chappell, J., Polach, H., Pillans, B. and Flood, P., 1986. Radiocarbon evidence for the timing and rate of island development, beach-rock formation and phosphatization at Lady Elliot Island, Queensland, Australia. *Marine. Geol.*, 69: 273-287.

Lady Elliot Island (Great Barrier Reef) is a coral cay constructed from near-concentric shingle ridges composed of coral, *Tridacna* shells and bioclastic sand bound by guano-derived phosphatic cement. Radiocarbon dating of individual *Tridacna* samples is used to investigate the evolution of the island and place constraints on the variations in storminess of the last 3200 years.

A shallow platform reef existed at Lady Elliot since at least 6500 yrs B.P. Shortly before 3200 yrs B.P. island growth by shingle progradation commenced and proceeded to the present at a rather uniform lateral rate (60 m ka^{-1} to leeward and 90 m ka^{-1} windward). Phosphatization may have occurred continuously or episodically at any time throughout the last 3200 years. The youngest cemented ridge top is less than 770 years, whereas at the base of uncemented ridges, phosphatization is a modern (~1950 A.D.) process. Similarly, low-level beach rock has continued to form within the last 25 years.

A significant period of instability occurred less than 500 years ago during which marine erosion truncated the southwestern extremity of Lady Elliot Island, formed an eastern "spit" and stranded high-level beach rock. However, the radiocarbon ages of *Tridacna* samples from shingle ridges from Lady Elliot and Curacoa Islands are uniformly distributed (Kolmogorov-Smirnov test) throughout the last 4000 years. We interpret this to indicate no significant variation in ridge-forming processes or fluctuation in average storminess during this interval.

INTRODUCTION

There is commonly difficulty in dating the development of Holocene storm-derived sand- and shingle-ridge sequences and their rates of progradation. Where these are composed of small shells or coral fragments, several pieces may be required to provide sufficient material for a single radiocarbon date. Results from the low and topographically subdued ridges of Nymph, Low-Wooded and West Hope islands (Chappell et al., 1983) in the northern Great Barrier Reef suggest that the wide assortment of radiocarbon "ages", from 2300 years B.P. to modern, results from reworking of materials by storm waves. In this case, it is also most probable that some individual "assemblages" of shells used for dating contained material with a variety of ages. McLean et al. (1978) have drawn attention to the wide range of ages (3000 years) for loose coral shingle on beaches from the Great Barrier Reef.

Similar difficulties have been encountered in attempting to date, by the C-14 method, episodes of tropical beach-rock formation (see review by Scoffin and Stoddart, 1983) and phosphatization (Stoddart and Scoffin, 1983).

In this study, we investigate aspects of these three problems using radiocarbon dates from individual large molluscs, *Tridacna maxima* and *T.gigas* cemented in shingle ridges, some of which were later phosphatized, and in beach rock. These shells are sufficiently large (12 to 30 cm across) to be dated as individuals and the consistency of the results presented hereunder suggests that these large shells from shingle ridges are more resistant to reworking than smaller shells and coral fragments. The C-14 dates thus provide maximum ages for the time of shingle-ridge and beach-rock formation.

GEOLOGICAL SETTING

Lady Elliot Island and reef (Fig. 1, lat. 24°07'S; long. 152°43'E) is the most southerly reef of the Great Barrier Reef province. The island (area 0.54 km^2, average height 4.5 m) is approximately 80 km from the Australian mainland and is exposed to the prevailing southeast Trade Wind. As described by Flood et al. (1979), the island is a coral cay (Fig.

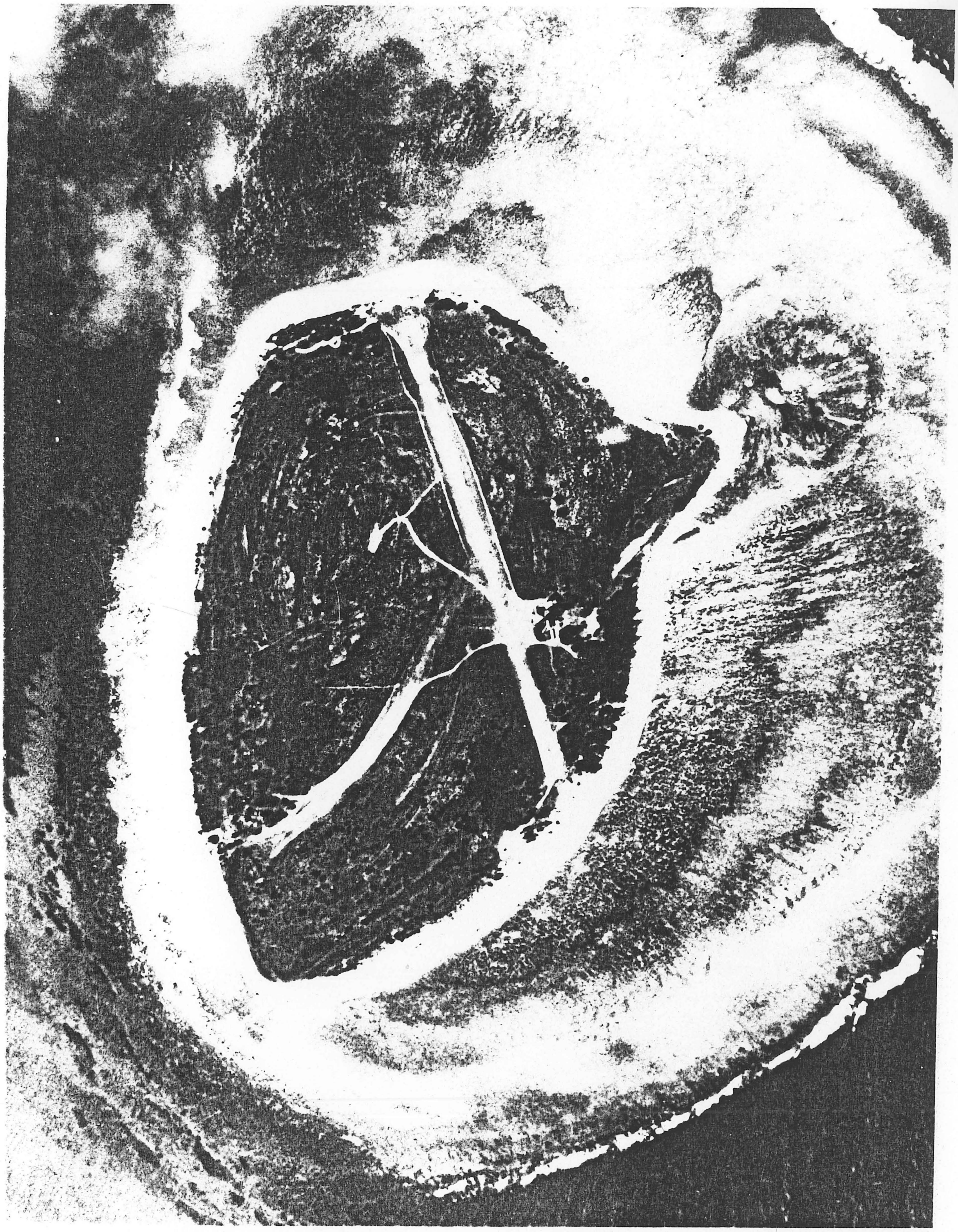

Fig. 1. Vertical aerial photograph (December 1982) of Lady Elliot Island and reef. Published with approval of the Royal Australian Air Force, Amberley, Queensland.

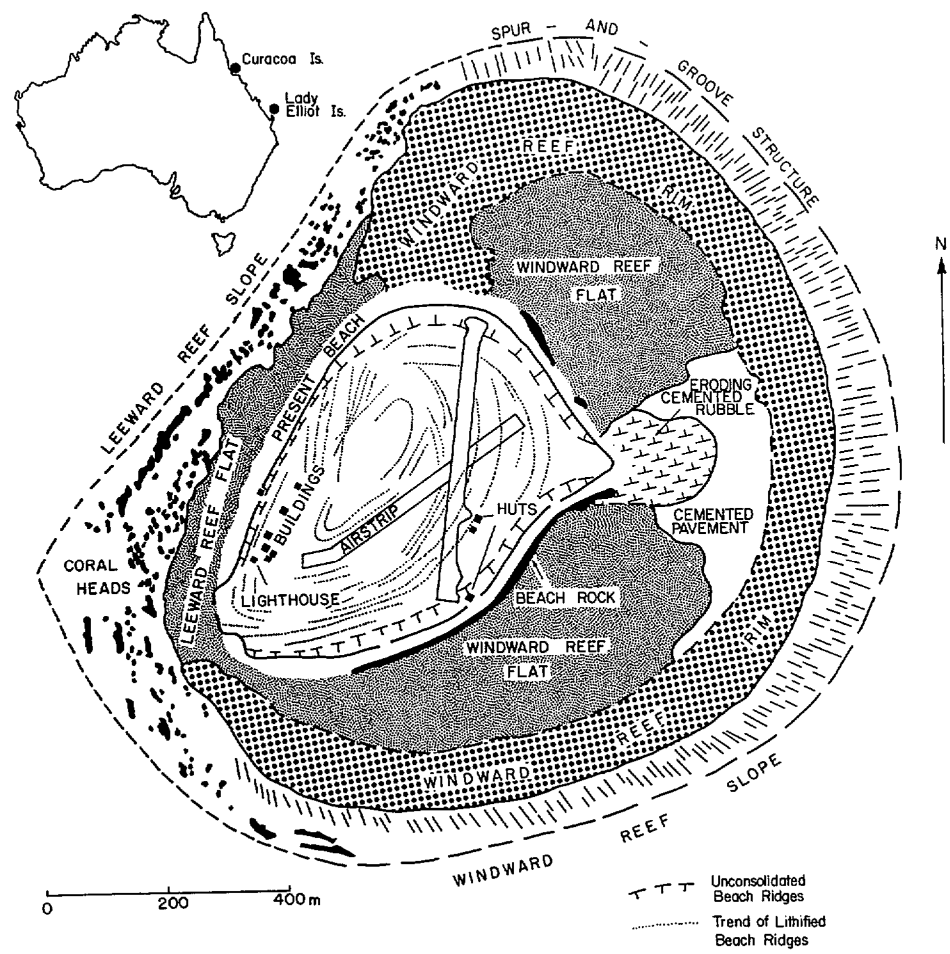

Fig. 2. Geomorphology of Lady Elliot Reef and Island (from Flood et al., 1979). Inset shows the location of Lady Elliot and Curacoa Islands near the Queensland coast.

2) comprising a near-concentric accumulation of prograded shingle ridges composed of coral, *Tridacna* shells and bioclastic sand bound together with a reddish-brown to cream coloured guano-derived phosphatic cement. Mining of phosphate between 1863 and 1873 led to almost total removal of the original vegetation and modification of the topography. In the central western part of the island some of the shingle ridges were removed; in the south western portion the topography appears to have been enhanced by excavations in the swales.

Between the modern sandy beach and the lithified ridges are from one to four uncemented shingle ridges which contain several pumice horizons. Intertidal exposed beach rock, commonly only a few centimetres thick, occurs along the eastern beaches. A small area of higher-level beach rock, approximately 1 metre above the intertidal beach-rock occurs on the easternmost point of the island.

Cemented and now-eroding cay rock occurs as pavements or platforms on the eastern and south western extremities of the island. The south western platform is stepped, with a lower level further offshore which may be a wave-cut feature. The eastern tongue of eroding cemented rubble lacks the phosphatic cement of the south western cay-rock and the inner shingle ridges.

SAMPLING PROCEDURE and RADIOCARBON RESULTS

Individual *Tridacna* were prised from lithified shingle ridges, beach rock, and cay-rock platforms. Sample sites and traverses are shown in Figures 3 and 4. Loose *Tridacna* were collected from the uncemented ridges. Clean portions of the shells were prepared by water-lubricated sawing and drilling to remove overgrowths and borings. Fifty-six new conventional C-14 ages (Table 1) are reported using the Libby ^{14}C half-life of 5568 years and corrected for the $^{13}C/^{12}C$ isotopic fractionation of the sample. The ages as discussed hereunder are corrected radiocarbon ages, obtained by subtracting 450±35 years, which represents the Australian oceanic reservoir effect (Gillespie and Polach, 1979). Fig. 3 also shows those previously published radiocarbon data from Lady Elliot Island - five dates from Flood et al. (1979) and four from Flood (1983). The previously reported dates (SUA-series) have been recalculated because $\delta^{13}C$ determinations are now available. Originally a $\delta^{13}C_{PDB}$ value of $0 \pm 2‰$ had been assumed for all samples.

Shingle-ridge sequences

Ages are reported for three surveyed sections, identified as A, B, and C (Figs. 3 and 4). Section A passes from an abandoned well, through the centre of the concentric ridge system at LE-49 (some 25 metres west of the well), to the west coast. The lower well

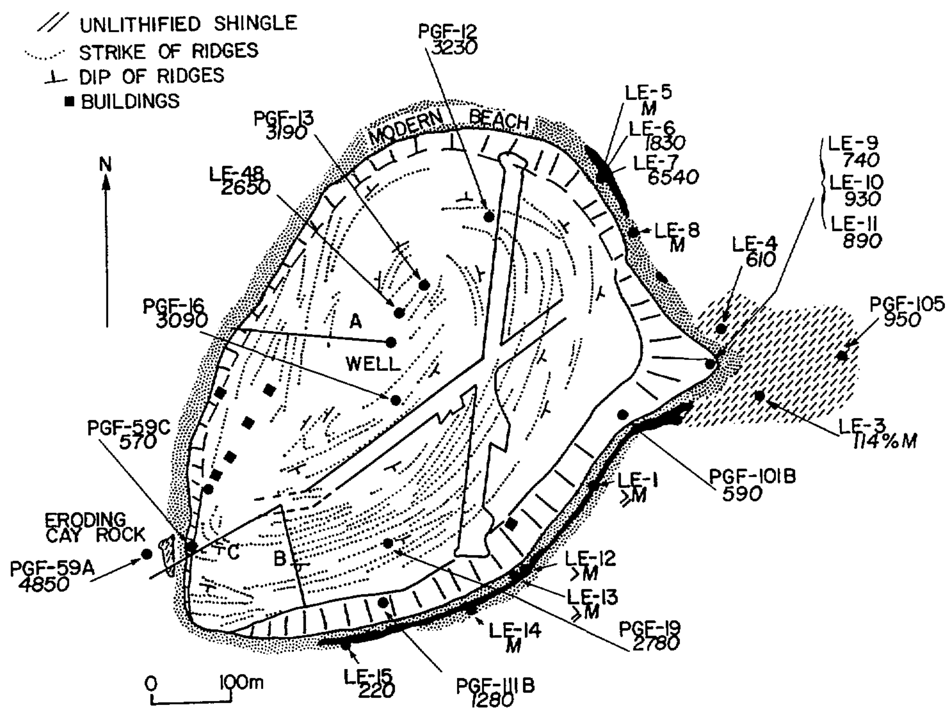

Fig. 3. Map of Lady Elliot Island showing locations of previous and new ^{14}C sample sites and surveyed sections. Sample numbers are followed by the corrected C-14 date. M = Modern. A, B, and C indicate the positions of the surveyed sections that are illustrated on Figure 4.

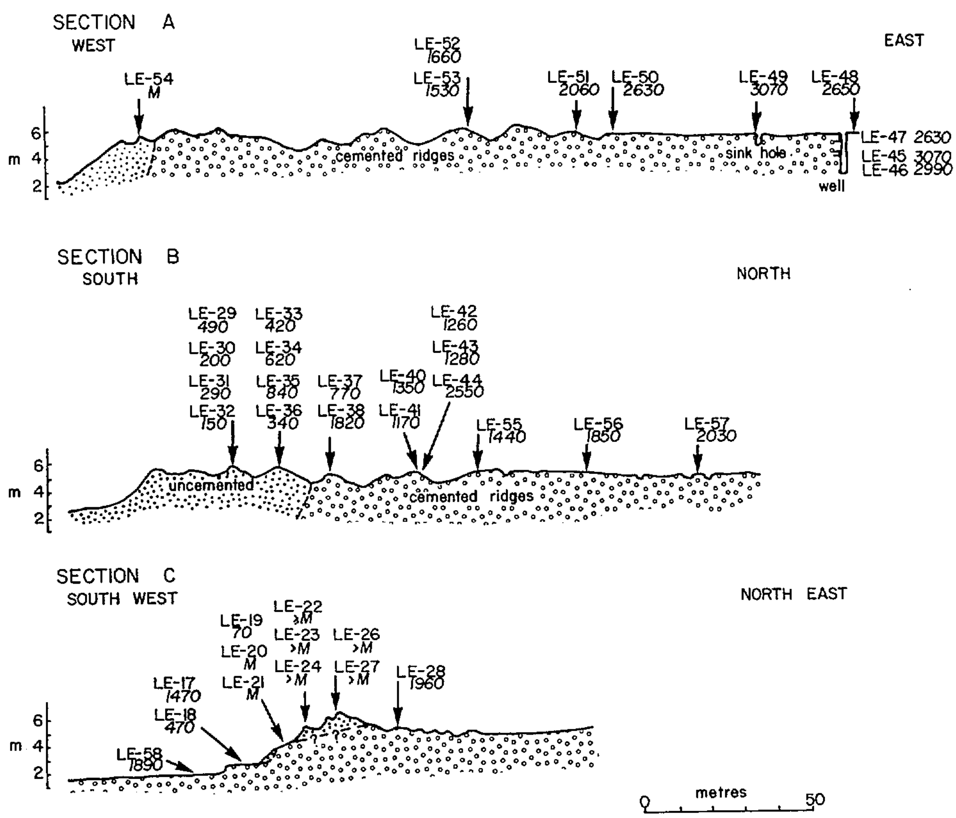

Fig. 4. Location and corrected ages of dated *Tridacna* samples from surveyed sections on Lady Elliot Island. Vertical scale indicates height above tidal prediction datum.

TABLE 1

Radiocarbon age results for *Tridacna* samples from Lady Elliot Island

Lab. code	Field code	Elevation (m)[a]	Notes	$\delta^{13}C_{PDB}$	Conventional ^{14}C age	Corrected ^{14}C age
Near centre of island						
SUA-861	PGF-LE-12		cemented	2.6	3680 ± 80	3230 ± 90
SUA-862	PGF-LE-13		cemented	2.2	3640 ± 80	3190 ± 90
SUA-863	PGF-LE-16		cemented	2.6	3540 ± 80	3090 ± 90
Section A						
ANU-3503	LE-47	4.5 (at top of well)	in well, depth 0.61 m	2.5	3080 ± 120	2630 ± 125
ANU-3502	LE-45		in well, depth 1.47 m	2.2	3520 ± 80	3070 ± 90
ANU-3498	LE-46		in well, depth 1.63 m	2.3	3440 ± 100	2990 ± 105
ANU-3486	LE-48		30 m north of well, cemented	1.4	3100 ± 100	2650 ± 105
ANU-3490	LE-49	4.35	at sink hole, cemented	2.0	3520 ± 80	3070 ± 90
ANU-3466	LE-50	~4.5	cemented	2.2	3080 ± 80	2630 ± 90
ANU-3487	LE-51	~4.5	cemented ridge	1.8	2510 ± 70	2060 ± 80
ANU-3493	LE-52	4.9	cemented ridge	2.8	2110 ± 70	1660 ± 80
ANU-3456	LE-53	4.9	cemented ridge	2.7	1980 ± 90	1530 ± 100
ANU-3488	LE-54	4.55	uncemented ridge	3.0	460 ± 70	M
Section B						
ANU-3491	LE-57	4.1	cemented	3.3	2480 ± 80	2030 ± 90
ANU-3467	LE-56	4.25	cemented	2.8	2300 ± 70	1850 ± 80
ANU-3504	LE-55	4.3	cemented	2.1	1890 ± 70	1440 ± 80
ANU-3465	LE-42	4.4	cemented ridge	2.1	1710 ± 70	1260 ± 80
ANU-3463	LE-43	4.4	cemented ridge	1.8	1730 ± 70	1280 ± 80
ANU-3485	LE-44	4.4	cemented ridge	2.6	3000 ± 80	2550 ± 90
ANU-3455	LE-40	4.4	loose material	2.5	1800 ± 100	1350 ± 105
ANU-3475	LE-41	4.4	loose material	3.0	1620 ± 70	1170 ± 80
ANU-3474	LE-37	4.25	cemented ridge	2.7	1220 ± 90	770 ± 100
ANU-3476	LE-38	4.25	cemented ridge	2.1	2270 ± 70	1820 ± 80
ANU-3471	LE-33	4.9	uncemented ridge	2.1	870 ± 70	420 ± 80
ANU-3496	LE-34	4.9	uncemented ridge	2.3	1070 ± 70	620 ± 80
ANU-3464	LE-35	4.9	uncemented ridge	2.1	1290 ± 70	840 ± 80
ANU-3477	LE-36	4.9	uncemented ridge	2.5	790 ± 90	340 ± 100
ANU-3462	LE-29	4.8	uncemented ridge	2.4	940 ± 40	490 ± 50
ANU-3454	LE-30	4.8	uncemented ridge	2.0	650 ± 70	200 ± 80
ANU-3470	LE-31	4.8	uncemented ridge	2.5	740 ± 80	290 ± 90
ANU-3484	LE-32	4.8	uncemented ridge	2.3	600 ± 80	150 ± 90
SUA-864	PGF-LE-19		outer cemented ridge, 120 m NE of section B	2.3	3230 ± 80	2780 ± 90
SUA-1286	PGF-111B		inner uncemented ridge, 120 m NE of section B	2.8	1730 ± 85	1280 ± 95
Section C						
ANU-3469	LE-28	4.05	cemented ridge	2.9	2410 ± 70	1960 ± 80
ANU-3494	LE-26	5.1	uncemented ridge	1.7	104.1 ± 0.9 %M	>M
ANU-3453	LE-27	5.1	uncemented ridge	2.3	102.3 ± 0.6 %M	>M
ANU-3473	LE-22	4.1	uncemented ridge	2.3	230 ± 60	≥M
ANU-3480	LE-23	4.1	uncemented ridge	2.3	99.9 ± 0.8 %M	>M
ANU-3468	LE-24	4.1	uncemented ridge	2.6	111.7 ± 0.7 %M	>M
SUA-866	PGF-LE-59C	3.4	red rock	2.5	1020 ± 70	570 ± 80
ANU-3483	LE-19	3.4	red rock	3.1	520 ± 70	70 ± 80
ANU-3495	LE-20	3.4	red rock	2.7	440 ± 70	M
ANU-3472	LE-21	3.4	red rock	2.3	380 ± 90	M
ANU-3461	LE-17	1.6	higher platform, cay rock	2.5	1920 ± 100	1470 ± 105
ANU-3482	LE-18	1.6	higher platform, cay rock	1.0	920 ± 70	470 ± 80
ANU-3497	LE-58	0.7	lower platform, cay rock	2.4	2340 ± 80	1890 ± 90
SUA-865	PGF-LE-59A		*Porites* sp. in-situ coral 0.5 m above level of living corals	0 ± 2 (estimate)	5300 ± 90	4850 ± 100
Samples from beach rock, cemented pavement, etc.						
ANU-3460	LE-5	intertidal	low-level beach rock	2.4	330 ± 70	M
ANU-3448	LE-6	intertidal	low-level beach rock	2.4	2280 ± 70	1830 ± 80
ANU-3449	LE-7	intertidal	low-level beach rock	2.9	6990 ± 100	6540 ± 105
ANU-3450	LE-8	intertidal	low-level beach rock	2.6	270 ± 80	≥M
ANU-3459	LE-1	intertidal	low-level beach rock	1.5	220 ± 70	≥M
ANU-3478	LE-12	intertidal	low-level beach rock	0.7	98.5 ± 0.6 %M	>M
ANU-3451	LE-13	intertidal	low-level beach rock	2.9	230 ± 40	≥M
ANU-3479	LE-14	intertidal	low-level beach rock	2.3	420 ± 70	M
ANU-3452	LE-15	intertidal	low-level beach rock	2.1	670 ± 70	220 ± 80
ANU-3492	LE-9		high-level beach rock	2.8	1190 ± 70	740 ± 80
ANU-3499	LE-10		high-level beach rock	2.4	1380 ± 80	930 ± 90
ANU-3481	LE-11		high-level beach rock	2.5	1340 ± 50	890 ± 60
ANU-3489	LE-4		eroding cemented rubble	2.6	1060 ± 70	610 ± 80
SUA-1285	PGF-105		eroding cemented rubble	1.7	1400 ± 85	950 ± 95
SUA-1284	PGF-101B		uncemented ridge near east point	2.6	1040 ± 60	590 ± 70
ANU-3447	LE-3		loose, dead, articulated *Tridacna*	1.6	114.3 ± 0.9 %M	>M
ANU-3457	LE-59		live coral (October 1982)	2.3	117.9 ± 1.0 %M	>M
ANU-3458	LE-60		live *Tridacna* (October 1982)	2.3	118.5 ± 0.9 %M	>M

[a] Elevations relative to tidal prediction datum.
[b] ^{14}C ages corrected for environmental (sea water) effect by subtracting 450 ± 35 from conventional age (Gillespie and Polach, 1979).

samples (LE-45,46), LE-49 and previously published results for nearby surface samples establish an age of initial shingle accumulation for the oldest presently exposed ridges at or after about 3200 years B.P. Samples further west along the traverse indicate progressively younger maximum ages for ridge formation (2630, 2060, 1660 years). A *Tridacna* from a near-shore uncemented ridge gives a corrected C-14 date of 10 years, which is essentially modern, but probably pre-bomb (1957 A.D.) in age.

Section B which is near the southern margin of the island also displays a regular progression of ages. For the cemented ridges, the corrected and averaged dates for individual ridges are 2030, 1850, 1440, 1270, 770 years. For two ridges, there is clear evidence of some reworking of material or delay in transport of older material from the beach front. In the shingle ridge where four *Tridacnas* average 1270 years (1170, 1260, 1280, 1350 years), one in-situ specimen is considerably older at 2550 years. In the youngest cemented ridge, one sample is 770 years old, another is 1820 years. Four *Tridacnas* from the most landward uncemented ridge of section B, gave ages of 840, 620, 420 and 340 years and four *Tridacnas* from the immediately younger ridge had ages of 490, 290, 200 and 150 years.

Two previously reported radiocarbon dates for *Tridacna* samples that were located about 120 m northeast of, and along strike of section B do not correlate with the well defined pattern of ages from section B. The sample from a cemented ridge (SUA-864, age 2780 years) appears to be from the same ridge as that from which we obtained a *Tridacna* dated at 1440 years. The older age may indicate that the particular shell has been reworked. There is also a previously reported date of 1280 years from the innermost unconsolidated ridge. Reworking seems likely for this specimen (SUA-1286), as our ages for *Tridacna* from the same ridge are 840, 620, 420 and 340 years.

From section A which has a leeward aspect and section B (windward) there are sufficient dated *Tridacna* samples to establish long-term maximum progradation rates. Fig. 5 shows data for the two sections from Lady Elliot Island and compares these with results from a section from the leeward gravel spit on Curacoa Island (lat 18° 40'S; long 146° 32'E) in the central Great Barrier Reef (Curacoa data given by Chappell et al., 1983). For these examples, we derive maximum progradation rates of 60 m/ka for the leeward side of Lady Elliot Island during the last 3000 years and 70 m/ka for the last 2000 years on the windward margin. The latter figure rises to approximately 90 m/ka years for the same windward sequence at its maximum width, which is 200 m to the northeast of section B. For section B, we can suggest that the lateral accretion rate was initially faster, 100 m/ka from 2000 to 1170 yrs B.P. then 50 m/ka from 1170 yrs B.P. to present. However, this may be illusory, and would be nullified by the discovery of a *Tridacna* with an age of about 1000 years in the ridge which produced specimens with ages of 1170, 1260, 1280, 1350 and 2550 years.

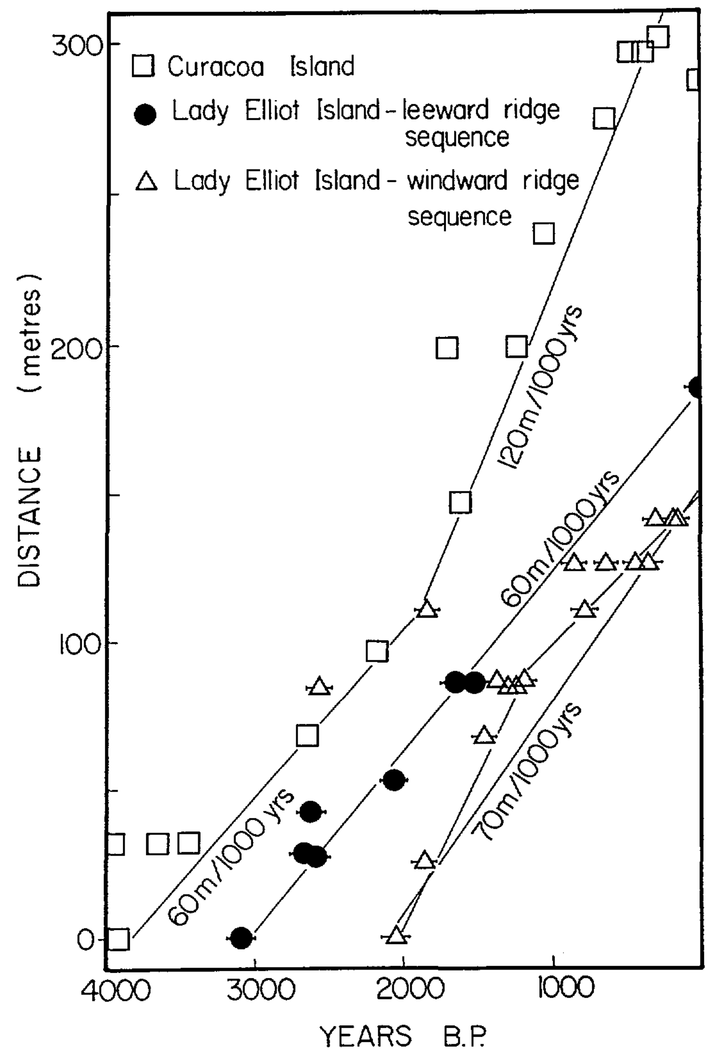

Fig. 5. Graphs of age of *Tridacna* specimens from shingle ridges as a function of progradation distance. Samples derived from the leeward (section A) and windward (section B) sequences of Lady Elliot Island. Also shown, for comparison, are results from the shingle-filled spit at Curacoa Island.

The sequence at Curacoa contains ridges composed of shingle and lithic clasts, the latter shed laterally from the continental island to which the spit is tied. The storm-ridge sequence which also has been dated using *Tridacna* and other molluscs (Chappell et al., 1983) spans the last 4,000 years and prograded at a mean maximum rate of 60 m/ka from 4000 to 2000 yrs B.P. then at 120 m/ka from approximately 2000 years B.P. to present.

Recent *Tridacna* remains are accumulating in the foreshore unconsolidated shingle ridges on Lady Elliot Island. Five samples from section C provided ages of ≥M(97.2), 99.9, 102.3, 104.1 and 111.7% modern, indicative of a bomb-^{14}C contribution. As a control, several very recent samples were analysed. An uncemented, dead but still articulated *Tridacna* offshore from the eastern extremity of the island had a ^{14}C activity equivalent to 114.3% modern. Live coral (*Goniastrea*) and *Tridacna* (both collected October 1982) from the eastern reef flat had ^{14}C activities of 117.9 and 118.5% modern, respectively.

Cay-rock pavements

Near the south western extremity of Lady Elliot Island (section C, Fig. 4), a *Tridacna* from the lower cay-rock platform has an age of 1890 years; two from the upper platform have ages of 1470 and 470 years. The step in the platform, which is parallel to the present shoreline, may be a wave-cut feature and/or the line of an original shingle ridge. The cay-rock is phosphate-cemented shingle debris and is thus compositionally similar to the cemented ridges elsewhere on the island. It is clear that the island was once more elongated towards the southeast and has been truncated by later erosion. On the southwestern tip of the island it is apparent, even from the map (Fig. 3), that older easterly-trending ridges are truncated perpendicularly by the present coastline and two modern unconsolidated storm ridges.

The youngest dated *Tridacna* from the southwestern cay-rock indicates that formation of a beach ridge, its cementation by phosphate, and subsequent marine erosion have all occurred in the last 470 years. Remnants of this ridge(s) now form an eroding cay rock beyond the present limit of the island.

The eroding cemented rubble on the eastern extremity of the island contains no phosphate cement. The shingle fragments are bound by algal cement and the mound is presently undergoing erosion. This accumulation is not unlike a spit that has formed from debris transported northwards by the prevailing winds from the southeastern reef flat. Two cemented *Tridacna* from the rubble have ages of 950 and 610 years, indicating accumulation in part since the last 600 years. This date (610±80) is indistinguishable from the maximum age (470±80) of erosion at the southwestern tip of island. It is possible that erosion in the southwest was broadly contemporaneous with deposition of debris as a diffuse spit on the eastern point of the island.

Phosphatization

Guano has provided the source of phosphate for cementation of the shingle ridges. At present, there is no large bird population and thus no new supply of phosphate. The decline of avian occupation may date from any time before or during the clearing of vegetation for phosphate mining operations (1863-1873 A.D.).

The outermost shingle ridges are not cemented by phosphate. The youngest dated *Tridacna* from a cemented ridge top is LE-37 with an age of 770 years. It is likely that the upper portions of the outermost ridges at any time would remain uncemented owing to wave action causing addition of new material and reworking of existing shingle. Such an environment may not be conducive to occupation by birds and therefore may lack phosphate.

There are *Tridacnas* younger than 770 years that are cemented by phosphate, but they are not from simple shingle ridge tops. A *Tridacna* cemented in the upper platform on the southwest extremity of the island has an age of 470 years. Above the modern beach at the same locality (Fig. 4, section C), exposed beneath the uncemented shingle foreridge, is an horizon of eroding shingle that is bound by poorly indurated phosphatic cement. At the time of sampling, this "red rock" had been exposed, perhaps only temporarily, by wave erosion that had cut well into the most shoreward uncemented shingle ridge. From this stratum, *Tridacnas* were recovered with ages ranging from 570 years to modern. One sample (LE-21) which has a C-14 activity that is ≥ modern may have a small bomb-^{14}C contribution. Thus phosphate cementation is presently occurring at the base of some uncemented ridges. The source of phosphate is probably not modern guano but may be derived by lateral migration of phosphate in solution from the inland shingle ridges.

The oldest phosphate-cemented *Tridacna* from the core of the island has an age of 3200 years. It is not possible to determine when phosphatic cementation of the inner ridges occurred. Avian occupation and phosphatization may have been continuous from 3000 years ago until last century. However, a shorter period or periods, for example with a duration(s) of a few hundred years at any time in the past 3000 years could produce the cemented ridges.

Beach rock

Several *Tridacnas* from the high-level beach rock on the eastern extremity of the island have corrected C-14 ages of 740, 890 and 930 years. Whereas these represent maximum ages of formation of this clearly older beach rock, the lack of younger clams supports an age of formation that may not be much younger than 700 years.

The ages of nine *Tridacna* that were cemented in the low-level beach rock that is under water at high tide, vary from 6500 years to greater than modern (i.e. post 1957 A.D.). Only three samples are pre-modern (ages of 6500, 1830 and 220 years), another two are modern and several show evidence of incorporation of bomb C-14. The low-level beach rock is clearly forming in the modern environment. The 6500-year old sample (LE-7) is a rounded clast of a *Tridacna* umbo with a long history of reworking in a high-energy environment prior to its incorporation in the modern beach rock.

DISCUSSION

Our results have implications for models of reef island formation, and for ideas about Holocene climatic variations. We consider formation of the shingle-ridge island first.

A shallow platform reef appears to have existed at Lady Elliot for at least 6500 years, indicated by the 6500-year old *Tridacna* (LE-7) within the modern beach rock at the northeast corner of the island. The 4850-year old *Porites* (PGF-LE-59A) near the southwest corner also shows early existence of the platform reef. All age results from shingle ridges, cayrock, and cemented rubble show no evidence for island formation before about 3200 years B.P., however. As outlined by Chappell (1982), and Chappell et al., (1983), island growth will not commence until the reef platform is sufficiently established by coral growth and sedimentation to provide a foundation close to sealevel. This stage probably was reached at Lady Elliot shortly before 3200 years ago.

Once initiated, the shingle ridges appear to have accreted concentrically (Figs. 2 and 3), with fairly constant ridge heights (Fig.4). Growth to windward and to leeward has occurred at rather similar uniform rates (Fig. 5). As the volume of shingle in the island is roughly proportional to the square of the radius of the island, the rate of volume accretion must increase with time. This might have two causes. Either the rate of shingle supply by reef growth increases with time; or the rate of shingle trapping per unit length of island perimeter is constant. The latter implies that the quantity of shingle derived from the reef and mobilized during a storm always exceeds the quantity which accretes to the island. Our data do not enable us to distinguish between these alternatives.

The second aspect for discussion concerns the possibility of late Holocene climatic or other fluctuations. Reef growth and ridge building conceivably can be affected by changes of sealevel, wave climate, and storm or cyclone frequency. We are concerned with the period since post-glacial sealevel rise terminated about 6000 years ago. The literature contains many papers in which sealevel oscillations or significant climatic fluctuations during the last 6000 years are claimed to have been recognized. In an earlier paper giving results from the central and northern Great Barrier Reef, we found no evidence for sealevel oscillations in the last 6000 years (Chappell et al., 1983). We also concluded that beach ridge sequences in the same region show no evidence for significant fluctuations of storminess.

Results from Lady Elliot Island have no sealevel information, because shingle ridges, cay rock, and beach rock can form at variable heights relative to tidal datum. Shingle ridge results are relevant for questions about fluctuations of storminess, however. Given that storm waves build new ridges, or distribute new material over previous ridges, shingle ridge ages can reveal whether or not storminess has fluctuated through time. If storm recurrence intervals remain statistically constant, then the ages of a series of prograded shingle ridges should be uniformally distributed through time. This is the null hypothesis. The alternative is that periods of greater-than-average storminess have occurred. This should be reflected by the existence of statistical "clumps" of shingle-ridge age results, separated by intervals with few or no age results.

The null hypothesis can be simply examined in two ways. The first is to see whether any particular interval has significantly more age results than the expected average. This test was applied by Chappell et al. (1983) to beach ridge data from the southern Gulf of Carpentaria, and from Princess Charlotte Bay and Curacoa Island in the northern and central Great Barrier Reef, respectively. After grouping ridge ages in successive 500-year intervals from 0 to 6000 years B.P., these authors concluded that no particular interval has anomalously many records (chi-square test), and the null hypothesis was accepted. The second technique is to graph the cumulative number of dates against time and examine the graph using the Kolmogorov-Smirnov test. This is the more powerful method and is used here.

Before discussing the time distribution of Lady Elliot age results, some points about our sampling are noted. Sampling traverses (Fig. 4) show that dated specimens were not uniformly spaced across the ridge sequence. Some ridges gave only a single sample, while several samples were collected from each of several other ridges. Offsetting this obvious sampling bias is the fact that age results indicate several episodes of accretion to any given ridge (e.g., the 4 northernmost ridges on Section B). Hence, sampling bias cannot be assessed but may be small.

Fig. 6 graphs the cumulative number of dates against sample age, arranged in ascending age order. All ridge-age results based on *Tridacna* are used, from SUA-861 down to ANU-3497 in Table 1, except for the five post-1957 AD results from Section C (shown as >M in Table 1). These are excluded because they are from the loose cap of modern shingle on Section C, giving an excessive number of >M data. The expected or null hypothesis curve representing uniform distribution of dates through time is shown as

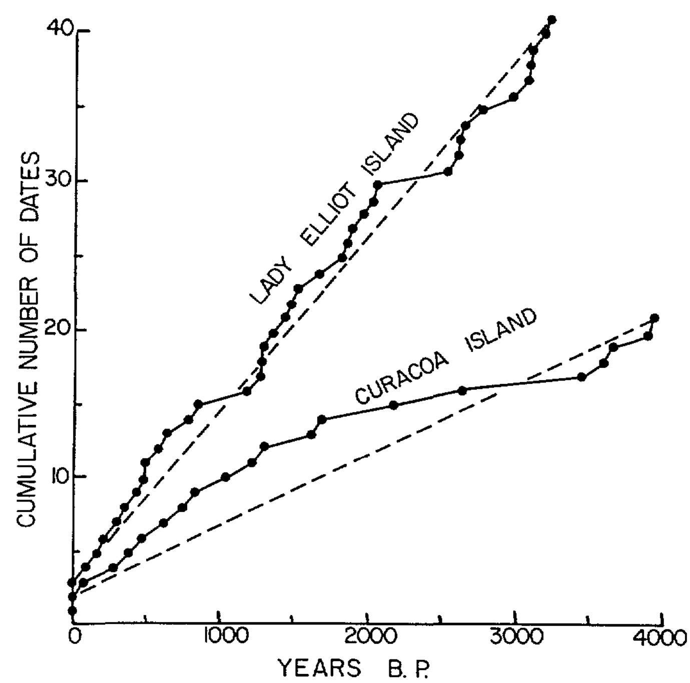

Fig. 6. Graph of radiocarbon ages of *Tridacna* samples from shingle ridges against cumulative number of samples taken in ascending age order, from Lady Elliot Island and from Curacoa Island. Dashed lines join highest-numbered modern-age sample and oldest-age sample in each case.

the dashed straight line in Fig. 6. For comparison, data from Curacoa Island in the central Great Barrier Reef (from Chappell et al., 1983) are similarly plotted in Fig. 6.

The Kolmogorov-Smirnov test proceeds by taking the maximum differences between observed and expected curves, illustrated in Fig. 6 for the Curacoa example. The K-S test statistic is d/n where n is number of observations. The method and tabulated significance levels of the K-S statistic are given by Siegel (1956). Applying the test to both Lady Elliot and Curacoa data in Fig. 6 shows that there is no significant difference between observed and expected distributions. Applying the test within segments of the curves also shows no significant differences except in the period between 1850 and 2540 B.P., where the clump of dates between 1850 and 2050 at Lady Elliot is mildly significant $[p(H_o) = 0.1]$. We note that this clump is not reflected in the Curacoa data. Taking the two data sets together, there is nothing visible in Fig. 6 to suggest any periods of significantly high, or low, frequency of ridge building. More sophisticated statistical analysis, in the hands of others, might eventually suggest clumping amongst these data. However, we conclude that the shingle ridge dates are uniformly distributed through time. We find no evidence for significant variations in storminess in the last 4000 years.

CONCLUSIONS

(1) Lady Elliot Island is composed of a series of prograded cemented shingle ridges that accumulated laterally at nearly uniform rates since about 3200 years B.P. The windward and leeward sequences had maximum mean lateral accumulation rates of 90 metres/ka and 60 metres/ka, respectively. The volumetric rate of accretion to the island as a whole has increased steadily through time.

(2) Marine erosion truncated the southwest extremity of the island, led to accumulation of algal-cemented rubble on the eastern tip of the island, and left residual high-level beach rock on the eastern peninsula. The high-level beack rock may have been once more widespread. These three features of marine erosion have been dated at less than 470,<610, and <740 years respectively and may have been broadly contemporaneous.

(3) Cementation of shingle ridges by guano-derived phosphate may have occurred at any time throughout the last 3200 years, in either a continuous or episodic manner. The youngest phosphate-cemented ridge top has an age less than 770 years. Phosphatization has continued until the present (~1950 A.D.) in the base of some uncemented ridges, perhaps by lateral as much as vertical solution movement.

(4) Low-level intertidal beach rock that crops out extensively along the eastern beaches formed in the last 25 years. *Tridacnas* cemented in the beach rock exhibit a variety of ages and include one rounded clast that has been reworked in the near-shore

environment for the last 6500 years. If beach rock is initially a subsurface formation, recent erosion is indicated.

(5) Radiocarbon ages of 41 *Tridacna* samples from the shingle ridges are uniformly distributed throughout the last 3200 years. We interpret this to mean that there have been no statistically significant fluctuations in ridge-forming processes during this period, in particular, that there have been no fluctuations of average storminess. This is consistent with our previous conclusions from Curacoa Island and other sites in north Queensland.

ACKNOWLEDGEMENTS

Chivas and Chappell acknowledge support from Marine Sciences and Technologies Research Grant 80/0091. Flood acknowledges support from Great Barrier Reef Marine Park Authority augmentative research grant 79/1. We are grateful for the contributions to laboratory work made by Cecily Vlastuin, John Head, Steve Robertson and Lynn Bell and for draughting by Joan Cowley.

REFERENCES

Chappell, J., 1982. Sealevels and sediments; some features of the context of coastal archaeologic sites in the tropics. Archaeology in Oceania, 17:69-78.

Chappell, J., Chivas, A., Wallensky, E., Polach, H.A. and Aharon, P., 1983. Holocene palaeo-environmental changes, central to north Great Barrier Reef inner zone. BMR J. Australian Geol. Geophys., 8:223-235.

Flood, P.G., 1983. Holocene sea level data from the southern Great Barrier Reef and southeastern Queensland - a review. In: D. Hopley (Editor), Australian sea levels in the last 15000 years: a review. Dept. of Geography, James Cook University of North Queensland, Occasional Paper 3:85-92.

Flood, P.G., Harjanto, S. and Orme, G.R., 1979. Carbon-14 dates, Lady Elliot Reef, Great Barrier Reef. Queensland Govt. Mining J., 80:444-447.

Gillespie, R. and Polach, H.A., 1979. The suitability of marine shells for radiocarbon dating of Australian prehistory. In: R. Berger and H. Suess (Editors), Radiocarbon Dating: Proceedings of the 9th International Conference on Radiocarbon Dating. Univ. California Press, Los Angeles and La Jolla, pp.404-421.

McLean, R.F., Stoddard, D.R., Hopley, D. and Polach, H., 1978. Sea level change in the Holocene on the northern Great Barrier Reef. Phil. Trans. R. Soc. Lond. A.291:167-186.

Scoffin, T.P. and Stoddard, D.R., 1983. Beachrock and intertidal cements. In: A.S. Goudie and K. Pye (Editors), Chemical Sediments and Geomorphology. Academic Press, London, pp.401-425.

Siegal, S., 1956. Non Parametric Statistics. McGraw Hill, New York, 312 pp.

Stoddard, D.R. and Scoffin, T.P., 1983. Phosphate rock on coral reef islands. In: A.S. Goudie and K. Pye (Editors), Chemical Sediments and Geomorphology. Academic Press, London, pp.369-400.

Chapter 3:
PHOSPHATE ROCK ON CORAL REEF ISLANDS

L.K. AYLIFFE, H.H.VEEH and A.R. CHIVAS

MODE OF OCCURRENCE AND GEOCHEMICAL CHARACTERISTICS

Phosphate deposits occur on numerous islands, especially in the Pacific and Indian oceans. Based on their composition and mode of occurrence, these deposits can be classified into three major groups:

(1) Guano, formed from the excreta of seabirds,

(2) Phosphatic calcarenites, consisting of carbonate sand or conglomerate cemented with apatite, and generally confined to low coral cays and atolls, and

(3) Deposits of more or less pure apatite, occurring on uplifted atolls, and usually resting on a limestone (dolomite) surface with well developed karst topography.

The deposits on low islands such as Lady Elliot Island appear to be quite young and are so closely associated with guano that a genetic relationship is almost certain, although the chemical reactions involved are complex and not fully understood.

Ancient deposits on high islands, of which Nauru is typical, can be of substantial size and have been the subject of past economic interest. Although it is widely assumed that these major deposits have also been derived from seabird guano, several of their characteristics are difficult to reconcile with such an origin. The sheer magnitude of some of the high-island deposits compelled Hutchinson (1950) to postulate the existence of unusual climatic and oceanographic conditions to enable their formation, such as high productivity in the surrounding sea (to sustain a large colony of seabirds) combined with prolonged periods of aridity (to preserve the guano), see Fig 1. Unfortunately, information on the absolute ages of these deposits are not readily available, making it difficult to correlate them with what is known of past environmental change. Aside from broad biostratigraphic time zones provided by the associated host limestones (i.e. Quaternary for Nauru to post Miocene for Makatea), only minimum ages of 200,000 years, based on uranium-series methods, are available for most of these ancient deposits.

A characteristic feature of these ancient deposits is evidence for extensive reworking, in terms of both physical redistribution as well as chemical reprecipitation of apatite, sometimes producing banded agate-like "nauruite".

The chemical composition of these major island deposits presents further difficulties in understanding their genesis. The relatively high concentrations of F and U commonly approach those of marine apatites. Since neither guano nor the limestone substrate contain sufficient F and U to be considered a likely source, several authors have proposed that these ancient deposits must have originated near sea level, exposed to sea spray and wave action, or within the confines of a lagoon of an emerging atoll receiving guano washed in from the surroundings.

THE PHOSPHATE OXYGEN TECHNIQUE AS A GEOCHEMICAL TRACER

The resistance of phosphate bound oxygen to isotopic-exchange in inorganic reactions at low temperatures (Tudge, 1960) should facilitate the tracing of phosphate along its path from seawater to final apatite deposition, and hence provide a critical test for choosing between the different models proposed for the origin of insular phosphorites.

Upon this premise samples of modern guano and insular phosphorites from a variety of locations and ages as well as associated phosphatic soils were analysed for their $\delta^{18}O_p$ compositions. The results of these analyses (summarised in Fig.2) provide new insights into the processes that control the formation of both modern and ancient insular phosphorite deposits.

Modern Guano

Bird guano is composed of both urine and fecal material, the phosphate contents of which are determined by the metabolic cycle of the bird and the phosphate content of the food supply. Phosphorus is required for protein metabolism and normally the rate at which it is lost via excretion in the urine will be matched by its rate of uptake in the intestine from ingested food. The guano-producing birds investigated feed predominantly on fish and squid, although the smaller birds, notably the Black Noddies, also eat crustaceans. Although some of the excreted phosphate in guano will have passed through the metabolic cycle of the bird, altering its initial $\delta^{18}O_p$ signature, the majority of guano phosphate will be determined by the birds' food source. The occurrence of poorly crystallised apatite, with an x-ray diffraction pattern similar to that of fishbone apatite, in most of the guano samples investigated supports this notion and suggests that the $\delta^{18}O_p$ signature of the guano should, to a large extent, be determined by that of the original food source, i.e. fishbone apatite in isotopic equilibrium with seawater.

The systematic relationship between $\delta^{18}O_p$-$\delta^{18}O_w$ and temperature for enzyme-mediated reactions under equilibrium conditions was originally determined by Longinelli and Nuti (1973) on the basis of phosphate inclusions in mollusc shells grown between 4 and 27 °C (Equation 1) and was subsequently confirmed by Kolodny et al. (1983), using fishbone apatite over the temperature range 3 - 15 °C:

$$T(^{o}C) = 111.4 - 4.3(\delta^{18}O_p - \delta^{18}O_w) \qquad (1)$$

where T is the mean temperature, and $\delta^{18}O_p$ and $\delta^{18}O_w$ are the oxygen isotopic signatures of phosphate and ambient water, respectively.

Fig. 2 is a graphical representation of this equation in terms of $\delta^{18}O_p$ and $\delta^{18}O_w$ for different temperatures, together with the measured $\delta^{18}O_p$ data of guano and apatite of various ages. In this plot, the implicit assumption is made that the sea surface temperatures at the respective sites have remained unchanged, in order to reconstruct $\delta^{18}O_w$ for the fossil apatite deposits.

Fig. 3 is consistent with the notion that temperature and $\delta^{18}O$ of seawater ($\delta^{18}O_w = 0$) are the major factors controlling the $\delta^{18}O_p$ values of guano samples. Possible variation produced by differences in seabird species and/or feeding habits must be comparatively small.

Phosphatic humus and Recent island phosphate rock

Recent and Late Pleistocene phosphatic calcarenites on low islands and the associated phosphatic soils have $\delta^{18}O_p$ signatures that are enriched with respect to contemporary guano. This relationship is well illustrated on both Lady Elliot Island and Heron Island where modern guanos are associated with an underlying raw acid humus and phosphatic hardpan. On Heron Island a phosphatic hardpan consisting of carbonate sand cemented with poorly crystallized apatite occurs at the contact between the acid humus and unconsolidated reef sand. The mode of occurrence of this phosphatic hardpan in the upper soil of Heron Island suggests that it is of very recent origin. It appears to be identical to the phosphatic hardpan described by Fosberg (1957) for many atolls of Micronesia, who considered an acid humus horizon to be crucial for the liberation of phosphate from guano, and hence for the subsequent formation of the phosphatic hardpan by chemical reaction between the phosphate and reef carbonate at an elevated pH. Radiocarbon ages of associated shingle ridges on Lady Elliot Island (Chivas et al., 1986) also infer a very recent origin for the phosphate deposition (< 3000 yrs B.P.). $\delta^{18}O_p$ of the phosphatic humus and underlying phosphatic hardpan at these two sites are about 2‰ lighter than associated guano (Fig. 3), indicating significant fractionation of oxygen isotopes in the course of transformation from guano to apatite under local environmental conditions.

It has been observed by several workers that micro-organisms such as bacteria are commonly involved in the degradation processes of guano. Should these microbes be active enough to cycle most of the phosphate present in the guano through their metabolic systems, then guano $\delta^{18}O_p$ could be reset according to $\delta^{18}O$ and temperature of local soil water. At a soil temperature of 24 °C, the measured $\delta^{18}O_p$ in the phosphatic hardpan would correspond to a $\delta^{18}O_w$ of +2.1‰ under equilibrium conditions (Equation 1). Isotopic enrichment of meteoric water in the unsaturated zone of soils due to evaporation from the soil surface has been demonstrated by Allison et al. (1983). Measurements of $\delta^{18}O$ in soil water at the same site on Heron Island where the phosphatic humus and hardpan were sampled (H.H Veeh and M.W. Hughes, unpublished data) confirms the existence of a well developed evaporation profile, except during or shortly after major precipitation events (Fig. 3). These data display an enrichment of the infiltrating meteoric water of more than 5‰ at the top of the soil profile and an enrichment of about 2‰ near the surface of the phosphatic hardpan i.e. at a depth of 7-12cm below the soil surface. Given this information, microbially mediated isotopic re-equilibration of guano $\delta^{18}O_p$ within the soil humus zone with near-surface waters of $\delta^{18}O = +2.1‰$ can readily explain the $\delta^{18}O_p$ of the phosphatic hardpan on Heron Island. Although not measured directly, soil waters on Lady Elliot Island are likely to be very similar to those on Heron Island, as are formation mechanisms.

If this reasoning is valid, similar processes must also govern the $\delta^{18}O_p$ signatures of apatite in other recent phosphate rock deposits. With the exception of the sample from Raine Island, all other phosphatic calcarenites, including the sample of Late Pleistocene age, reflect equilibration with waters which are significantly enriched in ^{18}O with respect to either seawater or local precipitation (Fig. 2). This supports the idea that the oxygen isotopic signature of apatite in phosphate rock is reset by bacterial means in the unsaturated zone of coral reef islands, presumably during leaching of phosphate from the guano. The unusually low $\delta^{18}O_p$ value of the apatite from Raine Island (sample RA-7) probably reflects its proximity to the monsoon-dominated rainfall province of S.E. Asia, known for its light $\delta^{18}O$ in precipitation.

Ancient high-island apatite deposits

In contrast to the relatively young phosphatic calcarenites from low coral reef islands, the major deposits of essentially pure apatite, generally found on emerged atolls such as Nauru, Ocean Island, Bellona or Makatea all have $\delta^{18}O_p$ signatures that are much lighter than their assumed modern precursors (Fig. 2). If these ancient apatites have not been affected by post depositional isotopic exchange, then their $\delta^{18}O_p$ reflect rather different processes and/or environments than those which govern $\delta^{18}O_p$ in modern deposits. Formation temperatures in excess of 40 °C are required for these ancient deposits if they have precipitated in equilibrium with waters of similar isotope compositions to those of the modern phosphorites (0 to +2‰ (SMOW)) (Fig. 2).

There is little doubt that most of the different types of apatite found in major island deposits are the result of extensive and repeated reworking processes following their initial emplacement. In fact, petrologic features consistent with deposition in the vadose zone appear to be characteristic of insular phosphorites in general .The spread of $\delta^{18}O_p$ for different types of apatite at one particular location (i.e. Nauru) probably reflects various stages in the diagenetic evolution of a given deposit, with numerous dissolution-reprecipitation cycles of the type described in great detail by Braithwaite (1980) on the basis of petrographic studies. In this connection it is worth noting that the sample with the most fractionated $\delta^{18}O_p$ signature is a "nauruite" with all the characteristics of a purely secondary late-stage precipitate.

It would seem therefore, that the isotopic composition of apatite in major insular phosphorites on high islands is the result of at least partial isotope exchange with meteoric water during their evolution from primary to secondary deposits in the course of weathering and supergene enrichment. Such enrichment processes have been well documented for sedimentary phosphorites elsewhere and appear to be typical of phosphorites associated with carbonates.

If isotope exchange between phosphate and meteoric water during weathering and diagenesis does take place, as suggested by our data, is this in conflict with the experimental evidence by Tudge (1960) that no isotopic fractionation between phosphate and water has been observed for inorganic processes at low temperatures? The most likely process by which such isotope exchange could be accomplished without violating this condition would be in association with microbial activity in the weathering environment. All microbes require a supply of inorganic phosphorus (usually as phosphate ions in solution) from their surrounding to meet the demands of cellular metabolic processes. Some micro-organisms are also capable of accessing normally unavailable sources of phosphate such as that bound in mineral Fe, Ca and Al - phosphates. Mechanisms employed by microbes to this end are many and varied: some produce organic and inorganic acids that directly dissolve these phases; some secrete chelating agents that complex the cations associated with these phosphate compounds and force their dissociation while others liberate phosphate from Fe-phosphates by the production of hydrogen sulphide. Indeed, Rodgers (1989) invokes the actions of sulphate-reducing bacteria, such as *Microspira desulfricans*, as a mechanism for the release of phosphate bound in soluble humic complexes within the soil profile of the atoll environment. Solubilisation of inorganic phosphate in soils by microbes has also been directly observed by Alexander (1964).

Thus it appears that the oxygen-isotope compositions of island phosphate deposits are subject to re-equilibration and/or isotope exchange with ambient water at virtually every stage, from initial emplacement at some primary site through several weathering and enrichment cycles under the influence of meteoric waters, to final preservation as essentially pure apatite. The determination of $\delta^{18}O_p$ in island phosphate promises to be a valuable research tool for the reconstruction of precipitation patterns and climate of the geologic past. It remains to be seen, however, to what extent the origin of insular phosphorites can be accurately defined by this method.

REFERENCES

Alexander, M., 1964. Introduction to soil microbiology, John Wiley & Sons, New York.

Allison, G.B., Barnes, C.J. and Hughes, M.W., 1983. The distribution of deuterium and ^{18}O in dry soils 2. Experimental, J. Hydrol. 64, 377-397.

Braithwaite, C.J.R., 1980. The petrology of oolitic phosphorites from Espirit (Aldabra), western Indian Ocean, Phil. Trans. R. Soc. London B 288, 511-543.

Chivas, A., Chappell, J., Polach, H., Pillans, B. and Flood, P., 1986. Radiocarbon evidence for the timing and rate of island development, beach-rock formation and phosphatization at Lady Elliot Island, Queensland, Australia. Marine Geology 69, 273-287.

Fosberg, F.R., 1957. Description and occurrence of atoll phosphate rock in Micronesia, Am. J. Sci. 255, 584-592.

Hutchinson, G.E., 1950. Survey of existing knowledge of biogeochemistry. 3. The biogeochemistry of vertebrate excretion. Bull. Am. Mus. Nat. Hist. 96, i-xviii, 1-554.

Kolodny, Y., Luz, B. and Navon, O., 1983. Oxygen isotope variations in phosphate of biogenic apatites, I. Fish bone apatite-rechecking the rules of the game, Earth Planet. Sci. Lett. 64, 398-404.

Longinelli, A. and Nuti, S., 1973. Revised phosphate-water isotopic temperature scale, Earth Planet. Sci. Lett. 19, 373-376.

Rodgers, K.A., 1989. Phosphatic limestones from Tuvalu (Ellice Islands), Econ. Geol. 84, 2252-2266.

Tudge, A.P., 1960. A method of analysis of oxygen isotopes in orthophosphate - its use in the measurement of paleotemperatures, Geochim. Cosmochim. Acta 18, 81-93.

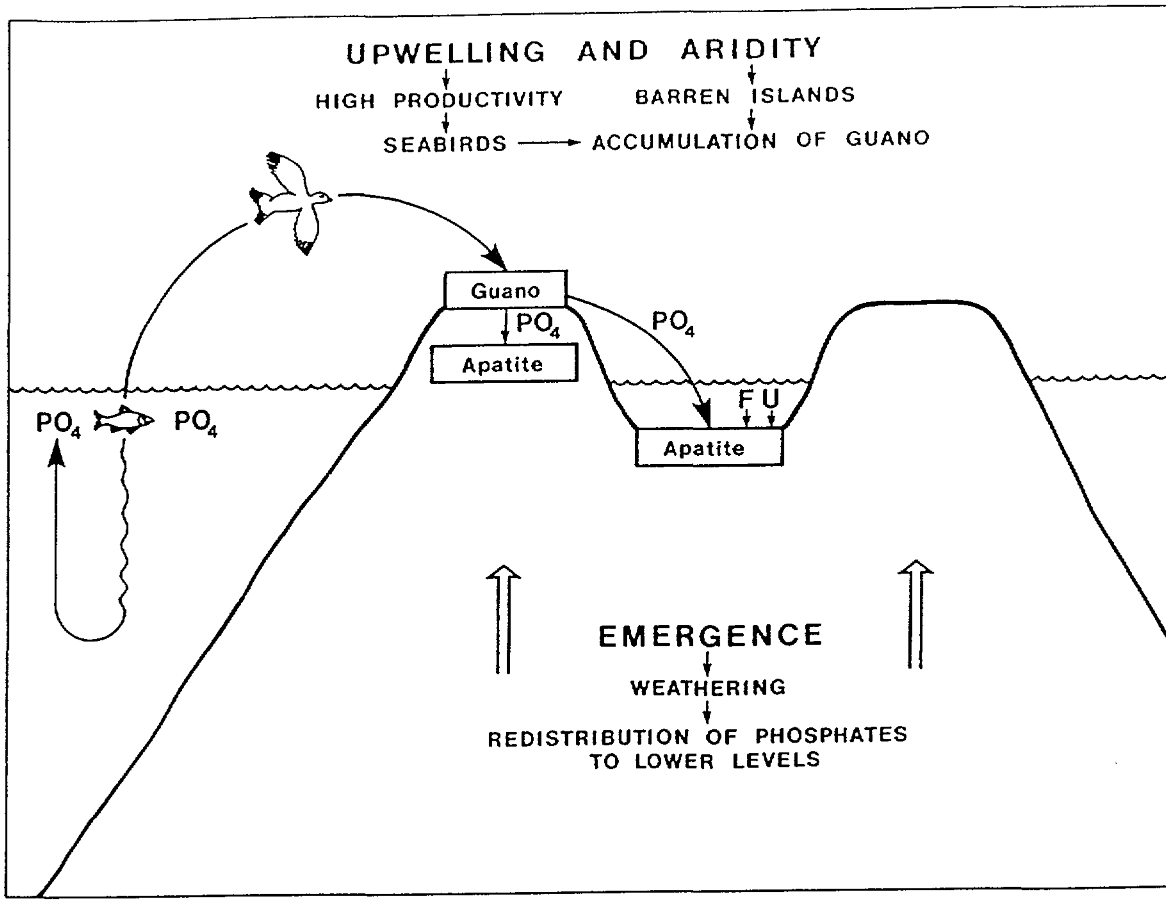

Figure 1.

Schematic model of phosphorite genesis on coral reef islands in terms of controlling parameters, and pathways of relevant elements. Two limiting cases for the depositional environment of insular phosphorites are shown. One case assumes phosphatization of reef limestone in the vadose zone of coral island interiors, with initially negligible U and F concentrations, the other case considers accumulation of guano derivatives in the shallow lagoon of an emerging atoll, and hence phosphatization in a marine ennvironment, with U and F concentrations approaching those of marine phosphorites.

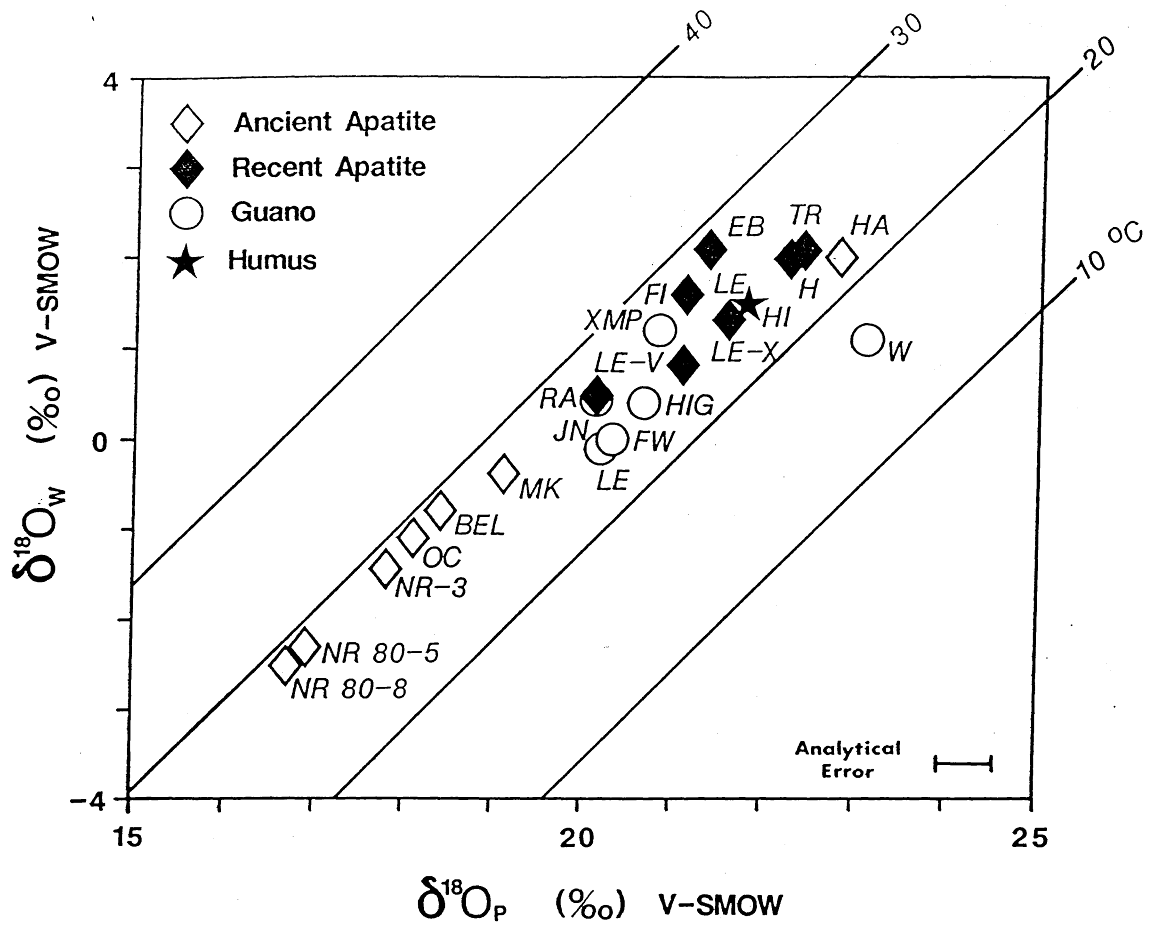

Figure 2.

Plot of $\delta^{18}O_p$, $\delta^{18}O_w$ and water temperature for the precipitation of phosphate under conditions of isotopic equilibrium, as derived by Longinelli and Nuti (1973);

$T(^oC) = 111.4 - 4.3(\delta^{18}O_p - \delta^{18}O_w)$. Guano and island apatite samples are plotted according to their measured $\delta^{18}O_p$ at present-day temperatures. Sample locations, descriptions, environmental temperatures and estimated ages are given in the following table.

Sample	Location	Type/Description	SST (°C)	Age
Guanos				
HIG	Heron Is.	Black Noddy	24.0	Modern
FWG	W. Fairfax Is.	Brown Booby	24.0	Modern
LE	Lady Elliot Is.	Black Noddy	24.0	Modern
JN	Johnston Is.	Red Footed Booby	26.5	Modern
XMP	Christmas Is.	Greater Frigate Bird	27.0	Modern
W	Winceby Is.	Cormorant	17.0	Modern
Phosphatic Soils				
H	Heron Is.	Phosphatic Humus	24.0	Modern
LE	Lady Elliot Is.	Phosphatic Humus	24.0	Modern
Recent and Late Pleistocene Phosphates				
TR	Tryon Is.	Phosphatic calcarenite	24.0	Recent
H	Heron Is.	Phosphatic hardpan	24.0	Modern
LE-V	Lady Elliot Is.	Phosphatic calcarenite, cgl.	24.0	<3000 yrs
LE-X	Lady Elliot Is.	Phosphatic calcarenite, cgl.	24.0	<3000 yrs
RA	Raine Is.	Phosphatic calcarenite	27.0	<1000 yrs
FI	Fanning Is.	Phosphatic calcarenite	27.5	≤4000 yrs
EB	Ebon Is.	Phosphatic calcarenite, cgl.	29.0	4000 yrs
HA	Pelsaert Is.	Partly phosphatised coral	22.0	112,000 yrs
Ancient Phosphates				
NR-3	Nauru	Phosphatised coral	29.0	>200,000 yrs
NR80-5	Nauru	Pisolitic phosphate sand	29.0	>200,000 yrs
NR80-8	Nauru	Nauruite	29.0	>200,000 yrs
OC	Ocean Is.	Pisolitic phosphate sand	29.0	>200,000 yrs
BEL	Bellona	Phosphate nodule	29.0	>200,000 yrs
MK	Makatea	Phosphate nodule	27.5	>200,000 yrs

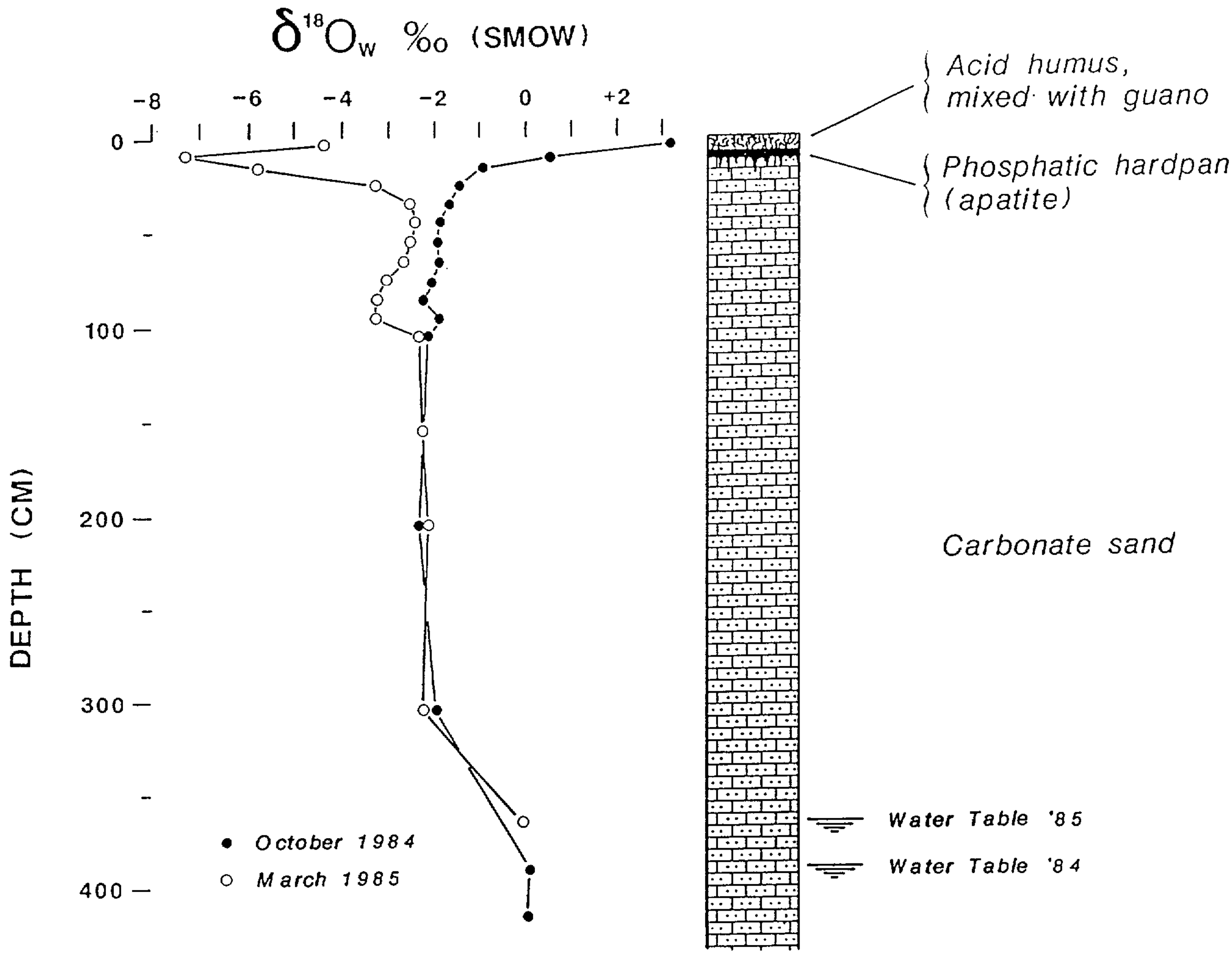

Figure 3.

Soil water $\delta^{18}O$ with depth from a site on Heron Island sampled in October 1984 and March 1985 (H.H. Veeh and M.W. Hughes, unpublised data), together with a schematic soil profile showing lithological change with depth.

REFERENCES CONCERNING CORAL FLUORESCENCE

Boto, K.G. and Isdale, P.J., 1985. Fluorescent bands in massive corals result from terrestrial fulvic acid inputs to nearshore zone. *Nature*, **315**, 396-397.

Isdale, P., 1984. Fluorescent bands in massive corals record centuries of coastal rainfall. *Nature*, **310**, 578-579.

Isdale, P.J. and Kotwicki, V., 1987. Lake Eyre and the Great Barrier Reef: a palaeohydrological ENSO connection. *South Aust. Geogr. J.*, **87**, 44-55.

Isdale, P.J. and Daniel, E., 1989. The design and deployment of a lightweight submarine fixed drilling system for the acquisition of coral cores. *Marine Technol. Soc. J.*, **23**, 3-10.

Klein, R., Loya, Y., Gvirtzman, G., Isdale, P.J. and Susic, M., 1990. Seasonal rainfall in the Sinai Desert during the Late Quaternary: evidence from fluorescent bands in fossil corals. *Nature*, **345**, 145-147.

Smith, T.J.III, Hudson, J.H., Roblee, M.B., Powell, G.V.N. and Isdale, P.J., 1989. Freshwater flow from the everglades to Florida Bay: an historical reconstruction based on fluorescent banding in the coral *Solenastrea bournoni*. *Bull. Marine Sci.*, **44**, 274-282.

Susic, M. and Isdale, P.J., 1989. A model for humic acid carbon export from a tropical river system using coral skeletal fluorescence data. In: Falconer, R.A., Goodwin, P. and Matthews, R.G.S. (eds), Hydraulic and Environmental Modelling of Coastal, Estuarine and River Waters. Gower Technical Press. Aldershot UK. pp 588-597.

Table: Comparison of ^{14}C and U/Th dates from coral samples from Lady Elliot Island

Field code	Coral species	Expected age (largely based on ^{14}C age of *Tridacna* in same or adjacent ridge)	$\delta^{13}C_{PDB}$ (‰)	Conventional ^{14}C age (yr B.P.)	U (ppm)	Th (ppm)	$^{234}U/^{238}U$	$^{230}Th/^{234}U$	U/Th age (yr)
LE-61 (repeat sampling of PGF-LE-59A	*Porites*	~5300 yr	1.0	4920 ± 80	2.03	0.033	1.130 ± 0.031	0.026 ± 0.002	2600 ± 200
LE-74	*Goniastrea*	~3500 yr	1.1	3150 ± 80	2.80	0.026	1.155 ± 0.060	0.036 ± 0.002	3600 ± 200
LE-62	*Goniastrea*	~3000 yr	0.2	2700 ± 70	2.25	0.009	1.111 ± 0.028	0.032 ± 0.0014	3200 ± 150
LE-68	*Goniastrea*	~1000 yr	0.3	2760 ± 80	1.88	0.014	1.257 ± 0.027	0.027 ± 0.002	2700 ± 200
LE-73	(collected January, 1990)		2.1	112.3 ± 0.9%M	2.57	0.019	1.121 ± 0.020	0.004	<1000

^{14}C ages from ANU Radiocarbon Dating Laboratory

$\delta^{13}C$ determinations by Joe Cali (Environmental Geochemistry Group, Research School of Earth Sciences, ANU)

U/Th determinations (α-spectrometry) by Audrey Chapman (Environmental Geochemistry Group, Research School of Earth Sciences, ANU)

Appendix: Tides at Lady Elliot Island during ICOG-7 field trip

Thursday 20 September, 1990	1000	high tide
	1600	low tide
Friday 21 September, 1990	1030	high tide
	1700	low tide
Saturday 22 September, 1990	1100	high tide
	1800	low tide

Appendix: Participants in ICOG-7 field trip to Lady Elliot Island

Ayliffe, Ms Linda Kay	Research School of Earth Sciences, Australian National University, Canberra
Chen, Dr James	California Institute of Technology, Division of Geol. & Planet Science, Pasadena California
Chivas, Allan R.	Research School of Earth Sciences, Australian National University, Canberra
Doe, Dr Bruce R. and wife (Margie)	US Geological Survey, 923 National Center, Reston Virginia
Flood, Peter G.	Department of Geology, The University of New England, Armidale
Goodfellow, Dr Wayne David	Geological Survey of Canada, Ottawa
Ikeda, Ms Sumiko	Department of Physics, Faculty of Science, Osaka University, Toyonaka
Ito, Mr Takashi	Department of Geoscience, The University of Tsukuba, Tsukuba, Ibaraki
Kamioka, Mr Hikari	Geological Survey of Japan, Tsukuba
Kasuya, Dr Masao	Department of Physics, Faculty of Science, Osaka University, Toyonaka
Muller-Sohnius, Dr Dieter	Mineralogisch-Petrologisch Institute, University of Munich, Theresienstrasse
Roksandic, Mr Zarko	Bureau of Mineral Resources, Canberra
Stone, John O.H.	Research School of Earth Sciences, Australian National University, Canberra
Summons, Dr Roger Everett	Bureau of Mineral Resources, Canberra
Todt, Dr Wolfgang	Max-Planck Institut fur Chemie, Federal Republic of Germany
Van Calsteren, Dr Peter	Department of Earth Sciences, The Open University, Milton Keynes
Veeh, Dr Herbert	School of Earth Sciences, Flinders University Bedford Park
Veizer, Professor Ján	Institut für Geologie, Ruhr Universität, Bochum
Yim, Dr Wyss	University of Hong Kong, (currently at Department of Geology, Australian National University, Canberra

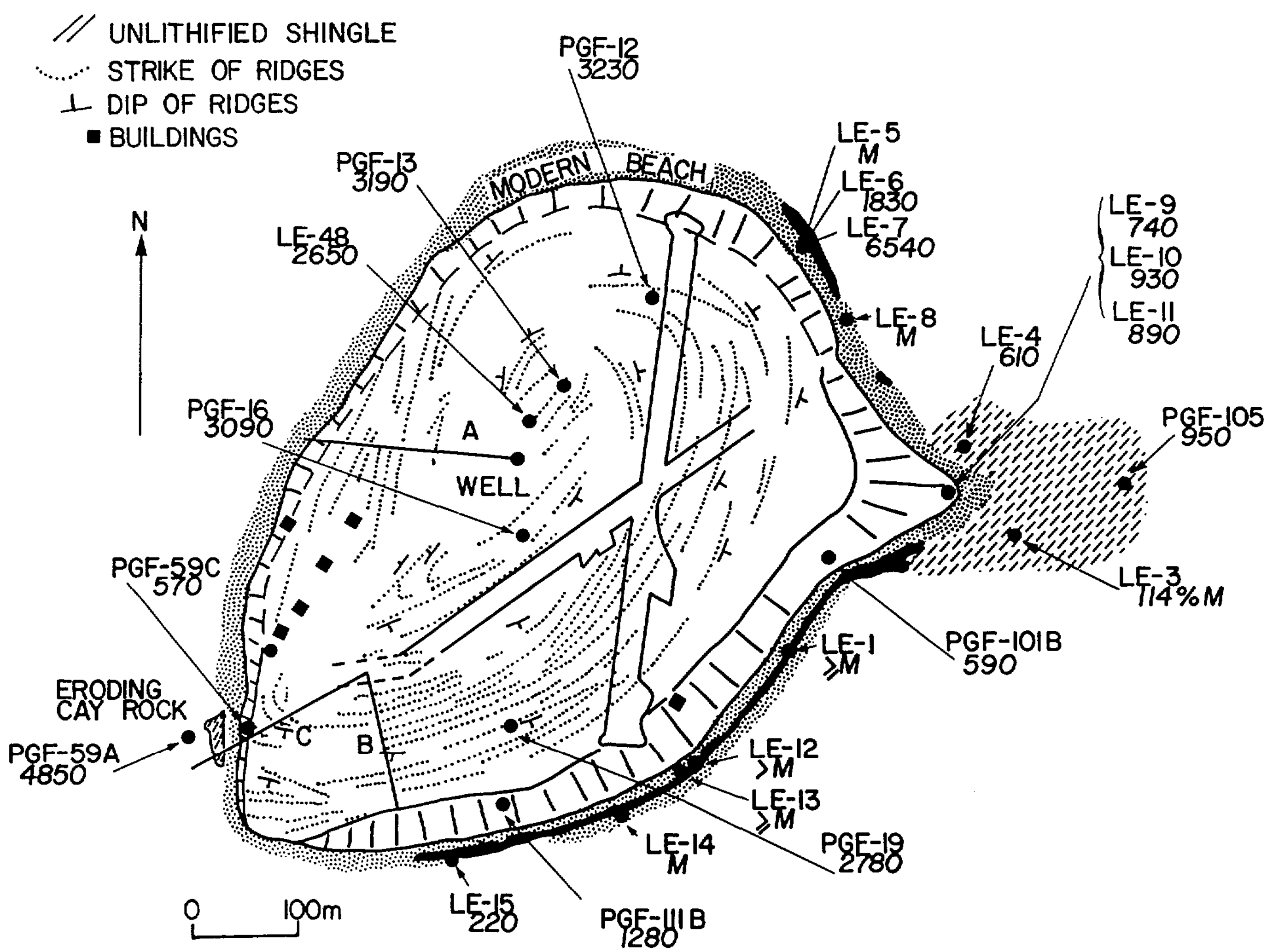

UNLITHIFIED SHINGLE
STRIKE OF RIDGES
DIP OF RIDGES
BUILDINGS
N
MODERN BEACH
PGF-12 3230
PGF-13 3190
LE-48 2650
LE-5 M
LE-6 1830
LE-7 6540
LE-8 M
LE-9 740
LE-10 930
LE-11 890
LE-4 610
PGF-105 950
LE-3 114%M
PGF-16 3090
A
WELL
PGF-59C 570
ERODING CAY ROCK
PGF-59A 4850
C
B
LE-1 ≥M
PGF-101B 590
LE-12 >M
LE-13 ≥M
PGF-19 2780
LE-14 M
LE-15 220
PGF-111 B 1280
0 100m

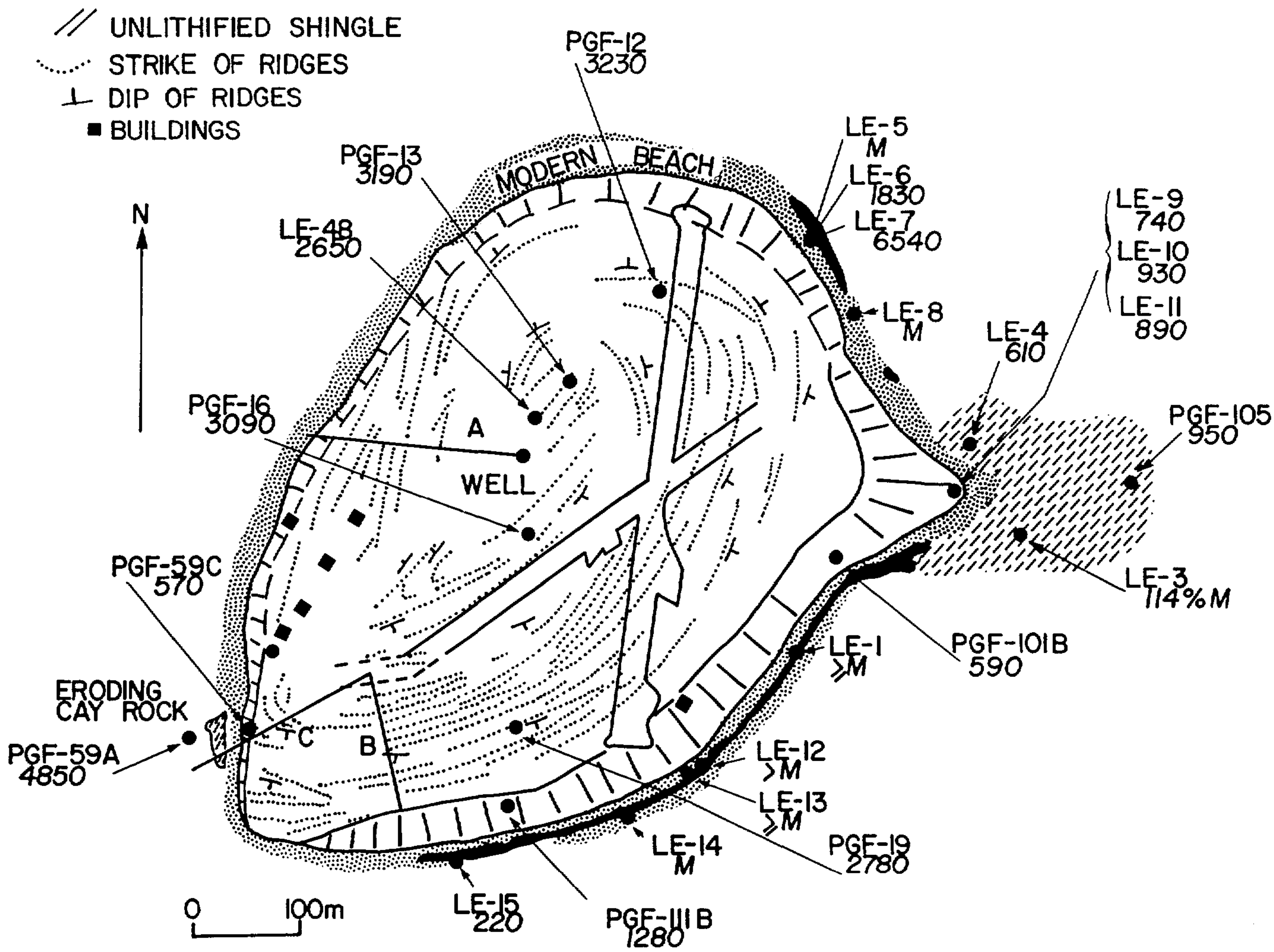
UNLITHIFIED SHINGLE
STRIKE OF RIDGES
DIP OF RIDGES
BUILDINGS
N
MODERN BEACH
PGF-12
3230
PGF-13
3190
LE-48
2650
LE-5
M
LE-6
1830
LE-7
6540
LE-8
M
LE-9
740
LE-10
930
LE-11
890
LE-4
610
PGF-105
950
PGF-16
3090
A
WELL
PGF-59C
570
ERODING
CAY ROCK
PGF-59A
4850
C
B
LE-3
114%M
PGF-101B
590
LE-1
>M
LE-12
>M
LE-13
>M
LE-14
M
PGF-19
2780
LE-15
220
PGF-111B
1280
0
100m